Magazine of Civil Engineering

ISSN 2712-8172

journal homepage: http://engstroy.spbstu.ru/

DOI: 10.34910/MCE.103.10

Bending of stiffened plates considering different stiffeners orientations

V. Pinto, M. Cunha, K. Martins, L. Rocha, E. Dos Santos, L. Isoldi*
Federal University of Rio Grande – FURG, Rio Grande, Brazil
** E-mail: liercioisoldi@gmail.com*

Keywords: stiffeners, geometric optimization, deflection, numerical simulation, computational modeling

Abstract. In engineering, the search for geometric configurations that lead to superior performance is always a design goal. Regarding structural components, such as plates, it is necessary to guarantee limits for its deflections, according to design standards. In this sense, methodologies devoted to reducing the out-of-plane displacements by geometric analysis are a relevant to subject research. Therefore, the present work is addressed to study several arrangements of stiffened steel plates defined by the Constructal Design Method (CDM). These plates were analyzed and solved applying computational modeling based on the Finite Element Method (FEM), aiming through the Exhaustive Search (ES) technique to evaluate the influence of stiffeners orientation on to the maximum deflection. Taking a non-stiffened plate as reference and keeping the total material volume constant, portions of its volume were transformed into stiffeners through the volumetric fraction parameter, representing the ratio between the volumes of stiffeners and reference plate. Adopting volumetric fraction values of 0.1; 0.2; 0.3; 0.4 and 0.5, it were established for each one 25 geometric arrangements of stiffened plates, considering the stiffeners orientations in 0 ° and 45 °, varying for each new arrangement the ratio between the height and thickness of the stiffeners h_s/t_s. The results showed that transforming a portion of material from a non-stiffened plate into stiffeners can decrease the maximum deflections by more than 95 %. Besides that, it has been demonstrated that stiffeners oriented at 45 ° can reduce maximum deflection by more than 60 % compared to stiffeners traditionally oriented at 0 °.

1. Introduction

Plates are flat and two-dimensional structural elements, whose main feature is the thickness much smaller than the width and length. Generally, the plates are subjected to loads that cause out-of-plane displacements. Those loads are transmitted in two directions, generating resistant bending, shearing and torsion efforts, allowing the plates to blend lightness and good load support capacity [1, 2].

Plates are broadly used in civil, aerospace and naval engineering. However, due to slenderness, it is usual to introduce reinforcements (stiffeners), in order to increase the flexural rigidity. The stiffeners can take on different cross section shapes and are traditionally welded to the plane of the plates in the longitudinal and/or transverse directions [3, 4].

In the analysis of non-stiffened thin plates, stresses and displacements can be obtained in a relatively simple way, using the classic Kirchhoff differential equation, applying for instance, Navier or Lévy solutions [3]. In its turn, regarding non-stiffened thick plates it is possible applying the Reisner's theory [5]. In addition, Ref. [6] indicates that the method based on the fundamental principles of the minimum of additional energy and possible displacements can be applied to solve both thin and thick non-stiffened plates.

Concerning stiffened plates, analytical solutions are unusual. Among the existing studies it is possible to quote Powell and Ogden [7] that proposed to idealize the stiffened plate into an equivalent orthotropic plate in order to analyze bridge decks.

However, analytical approaches for stiffened plates have limitations related to geometry, boundary conditions and loading, which can lead to inaccurate results. Thus, numerical methods become a good alternative that has been developed and applied by several researches over the past few years.

Rossow and Ibrahimkhail [8] applying the Constraint Method, studied the behavior of stiffened plates under uniform transverse loading with stiffeners in eccentric and concentric conditions, verifying their results using the Finite Element Method (FEM) by the NASTRAN® and STRUDL® software. Mukhopadhyay and Satsangi [9] used the FEM and developed a numerical model using isoparametric elements to analyze stiffened plates under bending, which made possible to insert the transverse shear deformations and curvature limits. Based on the energy principle, Kukreti and Cheraghi [10] presented an approach for stiffened plates where the deflection was determined by the product of polynomial and trigonometric series. Bedair [11] used Sequential Quadratic Programming (SQP) to analyze stiffened plates subject to uniform transverse loading, where the proposed model considered the system plate-stiffener rigidly connected. The Boundary Element Method (BEM) was applied by Tanaka et al. [12] to study the behavior of stiffened plates under bending, so that the forces and moments that interact in the plate-stiffener connection were treated as unknown variables and implemented in the numerical solution, being approximated through interpolation functions. In turn, the study proposed by Sapountzakis and Katsikadelis [13] used continuity equations to determine the forces that cause deflection and deformation between the plate-stiffener interface. In its turn, some numerical studies have been carried out seeking a better structural performance of stiffened plates. Singh et al. [14] used the ANSYS® software to perform a parametric analysis on stiffened plates under bending, considering different loads and boundary conditions. Also using the ANSYS® software, Troina et al. [15] applied the Constructal Design Method (CDM) allied to the Exhaustive Search (ES) technique for the analysis of different plate arrangements with orthogonal stiffeners in order to minimize the central deflection of stiffened plates.

More specifically, in structural engineering when it comes to the design of flat components subject to transverse loads, whether in metallic (present study) or reinforced concrete (e.g., slabs) structures, besides to ensure the safety, it is necessary to evaluate conditions of usability, for instance, to avoid deflections that are not in accordance with design standards. In this context, the development of methodologies related to the geometric evaluation dedicated to improving the mechanical performance of this kind of structure by means the minimization of its maximum deflection are relevant.

Given the above, the present study consists in the application of the CDM in a structural engineering component (stiffened steel plate), since this geometric evaluation method is a consecrated approach largely applied for heat transfer and fluid mechanics problems, however its application in mechanic of materials area it has not yet been properly investigated by the scientific community.

Therefore, as in Troina et al. [15], the present study applies CDM to define the geometric configurations of analyzed stiffened plates (search space), being the mechanical behavior of these plates numerically simulated through ANSYS® software. Finally, employing the ES technique, the geometric optimization of the stiffened plates was performed, aiming the minimization of the maximum deflection. It is important to highlight that there are three important differences in relation to the work of Troina et al. [15] which justify the research carried out here: i) the validation of proposed computational model by means of an experimental test; ii) the evaluation of the influence of stiffeners oriented at 45 °; and iii) the consideration of the maximum deflection as performance indicator.

2. Methods

2.1. Computational Modeling

Nowadays, computational modeling is an indispensable tool for analysis of complex engineering problems, enabling to test and extrapolate hypotheses till extreme values with safety and accuracy. The numerical methods, that are the basis of CAD tools (Computer-Aided Design), such as Finite Difference Method (FDM) and Finite Element Method (FEM), are applied in a range of scientific and industrial solutions that deal with analysis, optimization and development of products and projects [16, 17].

In this study, the FEM was adopted by means of the ANSYS® software. The finite element used to discretize all analyzed computational domains was the SHELL281 in the triangular version. This is a two-dimensional shell-type element, suitable for modeling thin plates, which has 6 nodes with 6 degrees of freedom per node: 3 rotations and 3 translations in relation to the *x*, *y* and *z* axes [18].

2.1.1. Computational Model Verification

The case used for computational model verification, as shown in Fig. 1, it was previously solved by Troina et al. [19] through ANSYS®, using the three-dimensional finite element SOLID95 in the hexahedral version.

The stiffened plate with a boundary condition of simply supported edges was subjected to a uniform transverse loading of 68.95 kPa and has material with an elastic modulus of 206.8427 GPa and Poisson's ratio of 0.3.

Here, the case was solved using the finite element SHELL281 in the triangular version, with a mesh that totaled 30,400 elements, defined according to the mesh convergence test presented in Fig. 2, where the result obtained by Troina et al. [19] is also presented.

Observing Fig. 2, it is possible to infer that the difference between the central deflection results U_z obtained in the present study of 0.281 mm and by Troina et al. [19] of 0.278 mm is 1.08 %, verifying the proposed computational model.

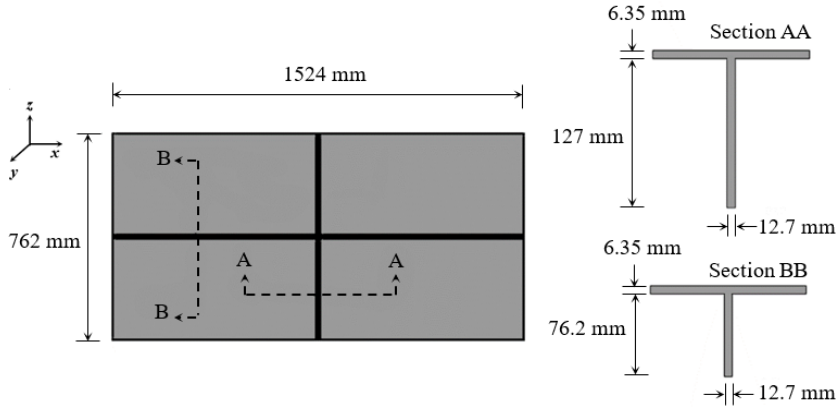

Figure 1. Rectangular plate with 2 orthogonal stiffeners.

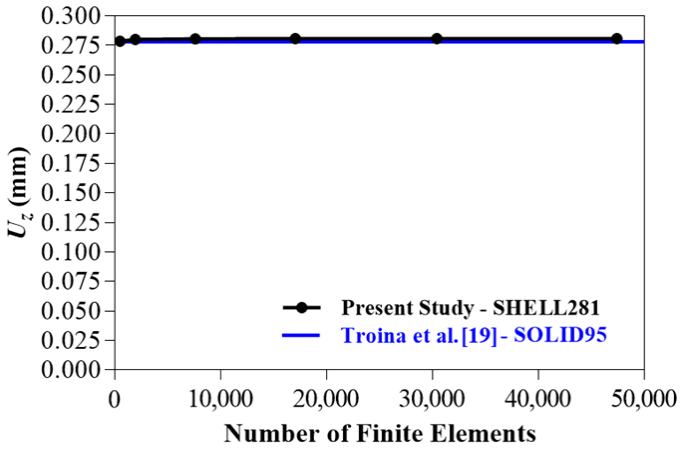

Figure 2. Computational model verification.

2.1.2. Computational Model Validation

The experimental test used for validation was presented by Carrijo et al. [20], as shown in Fig. 3. The square plate with eight stiffeners has an elastic modulus of 2.5 GPa and a Poisson's ratio of 0.36, being subjected to a uniform transverse load of 0.96 kPa. Concerning the boundary conditions, the plate is simply supported just on its four corners.

The experiment was numerically simulated using the finite element SHELL281 in its triangular version, with a mesh that totaled 5,070 elements, defined after the mesh convergence test presented in Fig. 4, which also shows the result found by Carrijo et al. [20].

Observing Fig. 4 it is possible to perceive that the difference for the central deflection U_z between the present study (6.505 mm) and the experimental results (6.220 mm) is 4.58 %, validating the computational model.

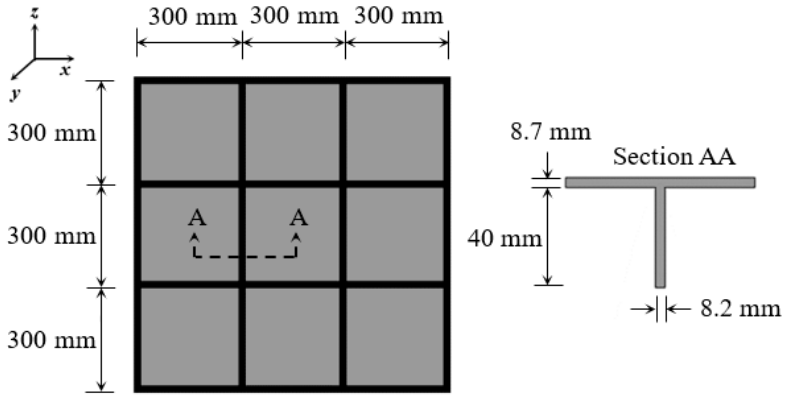

Figure 3. Square plate with eight stiffeners.

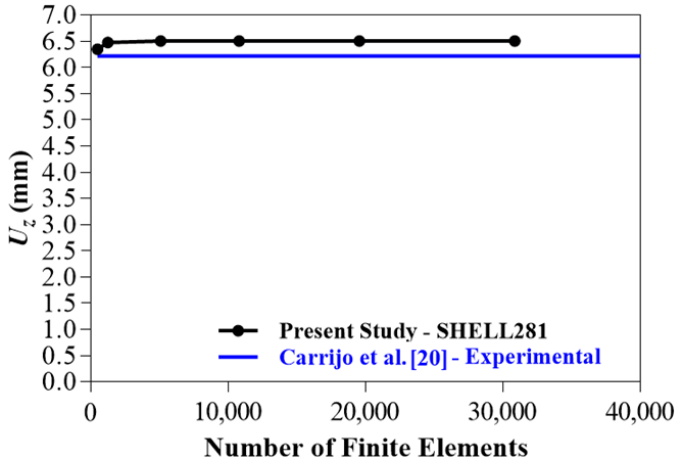

Figure 4. Computational model validation.

2.2. Constructal Design Method (CDM)

The physical phenomenon behind the vast geometric complexity of flow systems that occur in nature is called the Construct Law. These systems, whether animated or inanimate, tend to be imperfect, thus they evolve in time in order to distribute these imperfections in the best possible way, facilitating access to the currents that flow through them [21].

The performance of a flow system brings inherent restrictions, which can be, e.g., the space allocated for the development of the system, the material available and also limited rates of pressure, temperature or stress. The Constructal Design Method (CDM) is the practical application of the Constructal Law. Respecting the imposed restrictions, the degrees of freedom of the problem related to the geometric parameters are modified in order to assess its influence on a predefined performance indicator. Therefore, the CDM provides a guide for the designer to evaluate the flow system geometry, aiming to improve its performance, based on restrictions and objectives [22–24].

As earlier mentioned, the CDM is widely applied in problems of fluid mechanics and heat transfer, being possible to find several publications regarding these topics. However, in structural analysis, there are only a few studies employing the CDM, as in Bejan and Lorente [23], Lorente et al. [25] and Isoldi et al. [26], where the viability of its application in the analysis of structures was checked, analogously to applications in fluid mechanics and heat transfer.

Recently, some studies have proven the effectiveness of the CDM in structural applications: in the buckling analysis of perforated plates (Helbig et al. [27]; and Da Silva et al. [28]); in the buckling analysis of stiffened plates (Lima et al. [29] and Lima et al. [30]); in the bending analysis of stiffened plates (De Queiroz et al. [31]; Pinto et al. [32]); and Troina et al. [15]); and in the analysis of aircraft structures (Mardanpour et al. [33] and Izadpanahi et al. [34]).

To apply the CDM in this study, a non-stiffened steel plate with fixed dimensions was taken as reference: length a = 2000 mm, width b = 1000 mm and thickness t = 20 mm (thickness before transforming the volume portion into stiffeners). So, keeping the total material volume constant, as well as the dimensions a and b, different percentages of material deducted entirely from the thickness of this reference plate were converted into stiffeners through the volumetric fraction ϕ, which represents the ratio between the stiffeners

volume V_s and the reference plate volume V_r. So, five volumetric fractions values were adopted: ϕ = 0.1; 0.2; 0.3; 0.4; and 0.5; generated, respectively, by the t_p values of: 18 mm, 16 mm, 14 mm, 12 mm and 10 mm. Emphasizing that t_p is the thickness of the stiffened plates, i.e., after transforming the volume portion of the non-stiffened plate into stiffeners.

Regarding the stiffeners, two orientations were considered: 0° (not inclined, being positioned in the longitudinal and transverse directions), and 45° (inclined in relation to the plate edges). Because of that, the volumetric fraction ϕ for the 0 ° and 45 ° orientations are defined, respectively, by:

$$\phi = \frac{V_s}{V_r} = \frac{n_{sx}\left(ah_s t_s\right) + n_{sy}\left[\left(b - n_{sx}t_s\right)h_s t_s\right]}{abt} \tag{1}$$

$$\phi = \frac{V_s}{V_r} = \frac{\sum_{d=1}^{n}\left[\left(d_1 + d_2 + d_3 + Ld_n\right)h_s t_s\right] - \left(n_{int}h_s t_s^2\right)}{abt} \tag{2}$$

where h_s and t_s are, respectively, the height and thickness of the stiffeners. Exclusively for plate arrangements formed with stiffeners oriented at 45 °, the parameters d_1, d_2, d_3, ...d_n represent the length of the stiffeners, being n the total number and n_{int} the number of intersections. Moreover, to identify the plates arrangements, it was adopted the following format: P(n_{sx},n_{sy}) for plates with stiffeners oriented at 0° and P'($n_{sx'}$,$n_{sy'}$) for plates with stiffeners oriented at 45 °, being n_{sx} and n_{sy} the number of stiffeners in the x and y directions, as well as, $n_{sx'}$ and $n_{sy'}$ representing the number of stiffeners in the x' and y' directions. All of these parameters are shown in Fig. 5.

For each ϕ value, it were varied the degrees of freedom (stiffeners orientation, number of stiffeners and h_s/t_s ratio) defining the different geometric configurations which composes the search space. So, the plates were classified into groups according to the number of stiffeners, which varied from 2 to 6 in each direction (x, y and x', y'). The values of h_s/t_s ratio was consequence of the stiffeners heights h_s, established by Eqs. (1) and (2) for the different ϕ values, respecting each orientation, when different stiffeners thicknesses t_s were assigned (according to commercial plates thickness, in inches): $\frac{1}{8}$; $\frac{3}{16}$; $\frac{1}{4}$; $\frac{5}{16}$; $\frac{3}{8}$; $\frac{1}{2}$; $\frac{5}{8}$; $\frac{3}{4}$; $\frac{7}{8}$; 1; $1\frac{1}{4}$; $1\frac{1}{2}$; $1\frac{5}{8}$; $1\frac{3}{4}$; 2; $2\frac{1}{4}$; $2\frac{1}{2}$; and 3. The ranges of h_s/t_s variation can be identified in the graphs presented in the Figs. 11 to 35 and are exactly presented in Tables 1 to 5.

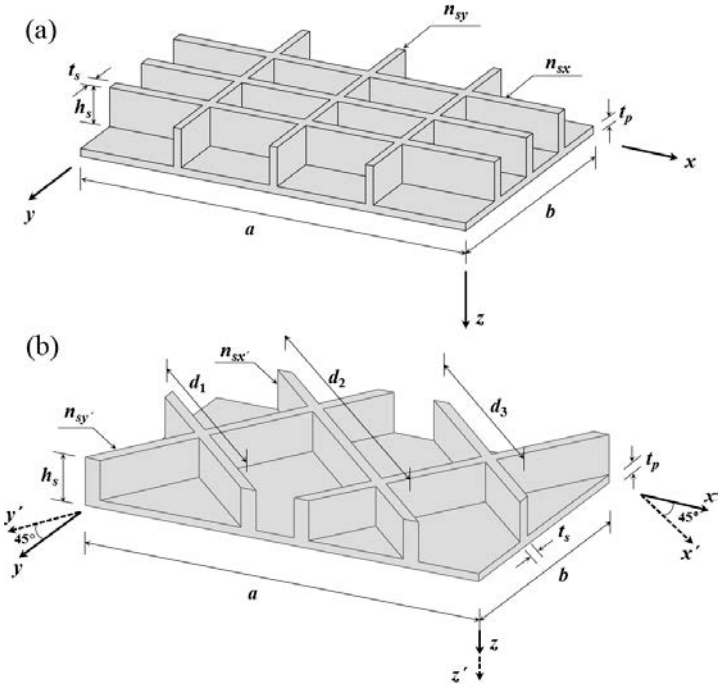

Figure 5. Geometric parameters of stiffened plates: (a) P(3,3); (b) P'(3,2).

Fig. 6 shows schematically the definition of the plate arrangements (search space) generated from the CDM application, which were numerically simulated in this study.

Table 1. Range of h_s/t_s for ϕ = 0.1.

Groups	P(n_{sx},n_{sy}) P'($n_{sx'}$,$n_{sy'}$)	h_s/t_s Range	
		Stiffeners Orientation	
		0°	45°
A	(2,2)	1.051 ≤ h_s/t_s≤ 66.065	1.106 ≤ h_s/t_s≤ 70.003
	(2,3)	1.182 ≤ h_s/t_s≤ 56.662	1.293 ≤ h_s/t_s≤ 62.280
	(2,4)	1.037 ≤ h_s/t_s≤ 49.602	1.117 ≤ h_s/t_s≤ 53.881
	(2,5)	1.230 ≤ h_s/t_s≤ 44.106	1.295 ≤ h_s/t_s≤ 46.721
	(2,6)	1.109 ≤ h_s/t_s≤ 39.706	1.181 ≤ h_s/t_s≤ 42.650
B	(3,2)	1.031 ≤ h_s/t_s ≤ 49.562	1.293 ≤ h_s/t_s ≤ 62.280
	(3,3)	1.228 ≤ h_s/t_s ≤ 44.091	1.558 ≤ h_s/t_s ≤ 56.091
	(3,4)	1.110 ≤ h_s/t_s ≤ 39.707	1.364 ≤ h_s/t_s ≤ 49.186
	(3,5)	1.012 ≤ h_s/t_s ≤ 36.116	1.199 ≤ h_s/t_s ≤ 43.150
	(3,6)	1.351 ≤ h_s/t_s ≤ 33.121	1.603 ≤ h_s/t_s ≤ 39.654
C	(4,2)	1.101 ≤ h_s/t_s ≤ 39.656	1.490 ≤ h_s/t_s ≤ 53.881
	(4,3)	1.006 ≤ h_s/t_s ≤ 36.085	1.364 ≤ h_s/t_s ≤ 49.186
	(4,4)	1.347 ≤ h_s/t_s ≤ 33.103	1.773 ≤ h_s/t_s ≤ 43.826
	(4,5)	1.248 ≤ h_s/t_s ≤ 30.577	1.584 ≤ h_s/t_s ≤ 38.993
	(4,6)	1.162 ≤ h_s/t_s ≤ 28.409	1.465 ≤ h_s/t_s ≤ 36.116
D	(5,2)	1.336 ≤ h_s/t_s ≤ 33.050	1.886 ≤ h_s/t_s ≤ 46.721
	(5,3)	1.240 ≤ h_s/t_s ≤ 30.539	1.745 ≤ h_s/t_s ≤ 43.150
	(5,4)	1.156 ≤ h_s/t_s ≤ 28.383	1.584 ≤ h_s/t_s ≤ 38.993
	(5,5)	1.084 ≤ h_s/t_s ≤ 26.511	1.418 ≤ h_s/t_s ≤ 35.061
	(5,6)	1.019 ≤ h_s/t_s ≤ 24.870	1.326 ≤ h_s/t_s ≤ 32.735
E	(6,2)	1.146 ≤ h_s/t_s ≤ 28.331	1.720 ≤ h_s/t_s ≤ 42.650
	(6,3)	1.075 ≤ h_s/t_s ≤ 26.471	1.603 ≤ h_s/t_s ≤ 39.654
	(6,4)	1.013 ≤ h_s/t_s ≤ 24.841	1.465 ≤ h_s/t_s ≤ 36.116
	(6,5)	1.492 ≤ h_s/t_s ≤ 23.399	2.072 ≤ h_s/t_s ≤ 32.735
	(6,6)	1.414 ≤ h_s/t_s ≤ 22.116	1.949 ≤ h_s/t_s ≤ 30.713

Table 2. Range of h_s/t_s for ϕ = 0.2.

Groups	P(n_{sx},n_{sy}) P'($n_{sx'}$,$n_{sy'}$))	h_s/t_s Range	
		Stiffeners Orientation	
		0°	45°
A	(2,2)	1.347 ≤ h_s/t_s ≤ 59.283	1.414 ≤ h_s/t_s ≤ 62.785
	(2,3)	1.162 ≤ h_s/t_s ≤ 50.860	1.268 ≤ h_s/t_s ≤ 55.882
	(2,4)	1.021 ≤ h_s/t_s ≤ 44.533	1.095 ≤ h_s/t_s ≤ 48.340
	(2,5)	1.418 ≤ h_s/t_s ≤ 88.213	1.488 ≤ h_s/t_s ≤ 93.443
	(2,6)	1.279 ≤ h_s/t_s ≤ 79.414	1.357 ≤ h_s/t_s ≤ 85.301
B	(3,2)	1.013 ≤ h_s/t_s ≤ 44.480	1.268 ≤ h_s/t_s ≤ 55.882
	(3,3)	1.414 ≤ h_s/t_s ≤ 39.585	1.792 ≤ h_s/t_s ≤ 50.347
	(3,4)	1.279 ≤ h_s/t_s ≤ 35.660	1.568 ≤ h_s/t_s ≤ 44.142
	(3,5)	1.168 ≤ h_s/t_s ≤ 72.232	1.379 ≤ h_s/t_s ≤ 86.300
	(3,6)	1.074 ≤ h_s/t_s ≤ 66.242	1.266 ≤ h_s/t_s ≤ 79.309
C	(4,2)	1.266 ≤ h_s/t_s ≤ 35.592	1.710 ≤ h_s/t_s ≤ 48.340
	(4,3)	1.159 ≤ h_s/t_s ≤ 32.402	1.568 ≤ h_s/t_s ≤ 44.142
	(4,4)	1.070 ≤ h_s/t_s ≤ 66.206	1.401 ≤ h_s/t_s ≤ 87.652
	(4,5)	1.293 ≤ h_s/t_s ≤ 61.154	1.637 ≤ h_s/t_s ≤ 77.986
	(4,6)	1.205 ≤ h_s/t_s ≤ 56.817	1.514 ≤ h_s/t_s ≤ 72.232

Groups	P(n_{sx},n_{sy}) P'($n_{sx'}$,$n_{sy'}$))	h_s/t_s Range	
		Stiffeners Orientation	
		0°	45°
D	(5,2)	$1.056 \le h_s/t_s \le 66.101$	$1.488 \le h_s/t_s \le 93.443$
	(5,3)	$1.281 \le h_s/t_s \le 61.079$	$1.801 \le h_s/t_s \le 86.300$
	(5,4)	$1.197 \le h_s/t_s \le 56.766$	$1.637 \le h_s/t_s \le 77.986$
	(5,5)	$1.124 \le h_s/t_s \le 53.022$	$1.463 \le h_s/t_s \le 70.122$
	(5,6)	$1.059 \le h_s/t_s \le 49.741$	$1.369 \le h_s/t_s \le 65.469$
E	(6,2)	$1.182 \le h_s/t_s \le 56.662$	$1.772 \le h_s/t_s \le 85.301$
	(6,3)	$1.112 \le h_s/t_s \le 52.943$	$1.653 \le h_s/t_s \le 79.309$
	(6,4)	$1.049 \le h_s/t_s \le 49.681$	$1.514 \le h_s/t_s \le 72.232$
	(6,5)	$1.320 \le h_s/t_s \le 46.798$	$1.823 \le h_s/t_s \le 65.469$
	(6,6)	$1.252 \le h_s/t_s \le 44.232$	$1.717 \le h_s/t_s \le 61.426$

Table 3. Range of h_s/t_s for ϕ = 0.3.

Groups	P(n_{sx},n_{sy}) P'($n_{sx'}$,$n_{sy'}$)	h_s/t_s Range	
		Stiffeners Orientation	
		0°	45°
A	(2,2)	$1.041 \le h_s/t_s \le 31.418$	$1.088 \le h_s/t_s \le 33.240$
	(2,3)	$1.042 \le h_s/t_s \le 42.747$	$1.135 \le h_s/t_s \le 46.951$
	(2,4)	$1.074 \le h_s/t_s \le 37.438$	$1.160 \le h_s/t_s \le 40.679$
	(2,5)	$1.367 \le h_s/t_s \le 59.409$	$1.431 \le h_s/t_s \le 62.891$
	(2,6)	$1.234 \le h_s/t_s \le 53.490$	$1.313 \le h_s/t_s \le 57.464$
B	(3,2)	$1.064 \le h_s/t_s \le 37.378$	$1.331 \le h_s/t_s \le 46.951$
	(3,3)	$1.362 \le h_s/t_s \le 33.278$	$1.733 \le h_s/t_s \le 42.353$
	(3,4)	$1.234 \le h_s/t_s \le 29.989$	$1.520 \le h_s/t_s \le 37.153$
	(3,5)	$1.128 \le h_s/t_s \le 48.666$	$1.332 \le h_s/t_s \le 58.129$
	(3,6)	$1.038 \le h_s/t_s \le 44.639$	$1.234 \le h_s/t_s \le 53.488$
C	(4,2)	$1.218 \le h_s/t_s \le 29.912$	$1.657 \le h_s/t_s \le 40.679$
	(4,3)	$1.118 \le h_s/t_s \le 27.243$	$1.520 \le h_s/t_s \le 37.153$
	(4,4)	$1.033 \le h_s/t_s \le 44.604$	$1.359 \le h_s/t_s \le 59.072$
	(4,5)	$1.489 \le h_s/t_s \le 41.213$	$1.893 \le h_s/t_s \le 52.577$
	(4,6)	$1.389 \le h_s/t_s \le 38.302$	$1.757 \le h_s/t_s \le 48.729$
D	(5,2)	$1.016 \le h_s/t_s \le 44.497$	$1.431 \le h_s/t_s \le 62.891$
	(5,3)	$1.474 \le h_s/t_s \le 41.137$	$2.075 \le h_s/t_s \le 58.129$
	(5,4)	$1.379 \le h_s/t_s \le 38.249$	$1.893 \le h_s/t_s \le 52.577$
	(5,5)	$1.295 \le h_s/t_s \le 35.740$	$1.686 \le h_s/t_s \le 47.228$
	(5,6)	$1.221 \le h_s/t_s \le 33.540$	$1.588 \le h_s/t_s \le 44.153$
E	(6,2)	$1.358 \le h_s/t_{s\ s} \le 38.145$	$2.046 \le h_s/t_s \le 57.464$
	(6,3)	$1.279 \le h_s/t_s \le 35.660$	$1.918 \le h_s/t_s \le 53.488$
	(6,4)	$1.209 \le h_s/t_s \le 33.480$	$1.757 \le h_s/t_s \le 48.729$
	(6,5)	$1.145 \le h_s/t_s \le 31.550$	$1.588 \le h_s/t_s \le 44.153$
	(6,6)	$1.089 \le h_s/t_s \le 66.348$	$1.504 \le h_s/t_s \le 92.275$

Table 4. Range of h_s/t_s for ϕ = 0.4.

Groups	P(n_{sx},n_{sy}) P'(n_{sx}',n_{sy}')	h_s/t_s Range	
		Stiffeners Orientation	
		0°	45°
A	(2,2)	1.070 ≤ h_s/t_s ≤ 29.550	1.116 ≤ h_s/t_s ≤ 31.248
	(2,3)	1.200 ≤ h_s/t_s ≤ 25.375	1.306 ≤ h_s/t_s ≤ 27.849
	(2,4)	1.057 ≤ h_s/t_s ≤ 31.502	1.126 ≤ h_s/t_s ≤ 34.144
	(2,5)	1.092 ≤ h_s/t_s ≤ 44.402	1.139 ≤ h_s/t_s ≤ 46.974
	(2,6)	1.155 ≤ h_s/t_s ≤ 39.985	1.216 ≤ h_s/t_s ≤ 42.873
B	(3,2)	1.045 ≤ h_s/t_s ≤ 22.180	1.306 ≤ h_s/t_s ≤ 27.849
	(3,3)	1.087 ≤ h_s/t_s ≤ 28.002	1.375 ≤ h_s/t_s ≤ 35.597
	(3,4)	1.155 ≤ h_s/t_s ≤ 25.242	1.407 ≤ h_s/t_s ≤ 31.199
	(3,5)	1.057 ≤ h_s/t_s ≤ 36.388	1.240 ≤ h_s/t_s ≤ 43.406
	(3,6)	1.385 ≤ h_s/t_s ≤ 33.385	1.623 ≤ h_s/t_s ≤ 39.881
C	(4,2)	1.137 ≤ h_s/t_s ≤ 25.161	1.531 ≤ h_s/t_s ≤ 34.144
	(4,3)	1.045 ≤ h_s/t_s ≤ 22.927	1.407 ≤ h_s/t_s ≤ 31.199
	(4,4)	1.377 ≤ h_s/t_s ≤ 33.349	1.799 ≤ h_s/t_s ≤ 44.088
	(4,5)	1.280 ≤ h_s/t_s ≤ 30.824	1.614 ≤ h_s/t_s ≤ 39.263
	(4,6)	1.195 ≤ h_s/t_s ≤ 28.655	1.491 ≤ h_s/t_s ≤ 36.356
D	(5,2)	1.354 ≤ h_s/t_s ≤ 33.243	1.908 ≤ h_s/t_s ≤ 46.974
	(5,3)	1.263 ≤ h_s/t_s ≤ 30.748	1.770 ≤ h_s/t_s ≤ 43.406
	(5,4)	1.184 ≤ h_s/t_s ≤ 28.602	1.614 ≤ h_s/t_s ≤ 39.263
	(5,5)	1.114 ≤ h_s/t_s ≤ 47.653	1.439 ≤ h_s/t_s ≤ 62.944
	(5,6)	1.052 ≤ h_s/t_s ≤ 44.720	1.348 ≤ h_s/t_s ≤ 58.778
E	(6,2)	1.162 ≤ h_s/t_s ≤ 28.498	1.738 ≤ h_s/t_s ≤42.873
	(6,3)	1.097 ≤ h_s/t_s ≤ 26.657	1.623 ≤ h_s/t_s ≤ 39.881
	(6,4)	1.038 ≤ h_s/t_s ≤ 25.039	1.491 ≤ h_s/t_s ≤ 36.356
	(6,5)	1.527 ≤ h_s/t_s ≤ 42.067	2.099 ≤ h_s/t_s ≤ 58.778
	(6,6)	1.452 ≤ h_s/t_s ≤39.775	1.980 ≤ h_s/t_s ≤ 55.169

Table 5. Range of h_s/t_s for ϕ = 0.5.

Groups	P(n_{sx},n_{sy}) P'(n_{sx}',n_{sy}')	h_s/t_s Range	
		Stiffeners Orientation	
		0°	45°
A	(2,2)	1.059 ≤ h_s/t_s ≤ 20.843	1.103 ≤ h_s/t_s ≤ 22.019
	(2,3)	1.158 ≤ h_s/t_s ≤ 17.909	1.258 ≤ h_s/t_s ≤ 19.642
	(2,4)	1.021 ≤ h_s/t_s ≤ 27.792	1.084 ≤ h_s/t_s ≤ 30.101
	(2,5)	1.181 ≤ h_s/t_s ≤ 35.034	1.229 ≤ h_s/t_s ≤ 37.038
	(2,6)	1.067 ≤ h_s/t_s ≤ 31.553	1.119 ≤ h_s/t_s ≤ 33.801
B	(3,2)	1.007 ≤ h_s/t_s ≤ 15.649	1.258 ≤ h_s/t_s ≤ 19.642
	(3,3)	1.174 ≤ h_s/t_s ≤ 24.704	1.484 ≤ h_s/t_s ≤ 31.397
	(3,4)	1.067 ≤ h_s/t_s ≤ 22.276	1.296 ≤ h_s/t_s ≤ 27.514
	(3,5)	1.130 ≤ h_s/t_s ≤ 28.722	1.323 ≤ h_s/t_s ≤ 34.234
	(3,6)	1.042 ≤ h_s/t_s ≤ 26.358	1.213 ≤ h_s/t_s ≤ 31.450
C	(4,2)	1.047 ≤ h_s/t_s ≤ 22.191	1.407 ≤ h_s/t_s ≤ 30.101
	(4,3)	1.116 ≤ h_s/t_s ≤ 20.230	1.501 ≤ h_s/t_s ≤ 27.514
	(4,4)	1.034 ≤ h_s/t_s ≤ 26.322	1.345 ≤ h_s/t_s ≤ 34.773
	(4,5)	1.126 ≤ h_s/t_s ≤ 24.338	1.417 ≤ h_s/t_s ≤ 30.983
	(4,6)	1.053 ≤ h_s/t_s ≤ 35.819	1.308 ≤ h_s/t_s ≤ 45.445

Groups	P(n_{sx},n_{sy}) P'($n_{sx'}$,$n_{sy'}$)	h_s/t_s Range	
		Stiffeners Orientation	
		0°	45°
D	(5,2)	$1.012 \le h_s/t_s \le 26.216$	$1.423 \le h_s/t_s \le 37.038$
	(5,3)	$1.109 \le h_s/t_s \le 24.262$	$1.550 \le h_s/t_s \le 34.234$
	(5,4)	$1.041 \le h_s/t_s \le 22.579$	$1.417 \le h_s/t_s \le 30.983$
	(5,5)	$1.392 \le h_s/t_s \le 33.420$	$1.799 \le h_s/t_s \le 44.088$
	(5,6)	$1.314 \le h_s/t_s \le 31.374$	$1.685 \le h_s/t_s \le 41.177$
E	(6,2)	$1.017 \le h_s/t_s \le 22.476$	$1.520 \le h_s/t_s \le 33.801$
	(6,3)	$1.371 \le h_s/t_s \le 21.035$	$2.029 \le h_s/t_s \le 31.450$
	(6,4)	$1.298 \le h_s/t_s \le 31.298$	$1.864 \le h_s/t_s \le 45.445$
	(6,5)	$1.233 \le h_s/t_s \le 29.507$	$1.685 \le h_s/t_s \le 41.177$
	(6,6)	$1.173 \le h_s/t_s \le 27.910$	$1.592 \le h_s/t_s \le 38.664$

Following the constraints indicated in Troina et al. [15], the heights of the stiffeners h_s were limited to 300 mm, avoiding excessive disproportion in relation to the dimensions of the plate; as well as, h_s/t_s ratios less than one were disregarded, preventing stiffeners thicknesses greater than heights.

It is important to mention that all stiffened plates analyzed in this study were considered as simply supported and subjected to a uniformly distributed transverse load equal to 10 kPa, aiming to guarantee a linear-elastic material behavior and a geometric linear structural analysis. To apply this type of load in the ANSYS® software, a pressure in the positive z direction over the plate surface was imposed. The material was structural steel A-36 with an elastic modulus of 200 GPa and Poisson's ratio of 0.3. Taking as example the stiffened plate P'(3.3), Fig. 7 illustrates how the boundary conditions and loading were imposed, while Fig. 8 show the discretization of the computational domain. These aspects were considered in a similar way for all other studied geometric configurations.

In addition, the simplifying hypothesis of ideal structures, i.e., the non-consideration of initial geometric imperfections was assumed for all simulated plates. This assumption ensures that the only difference among the studied plates is really its geometric configuration.

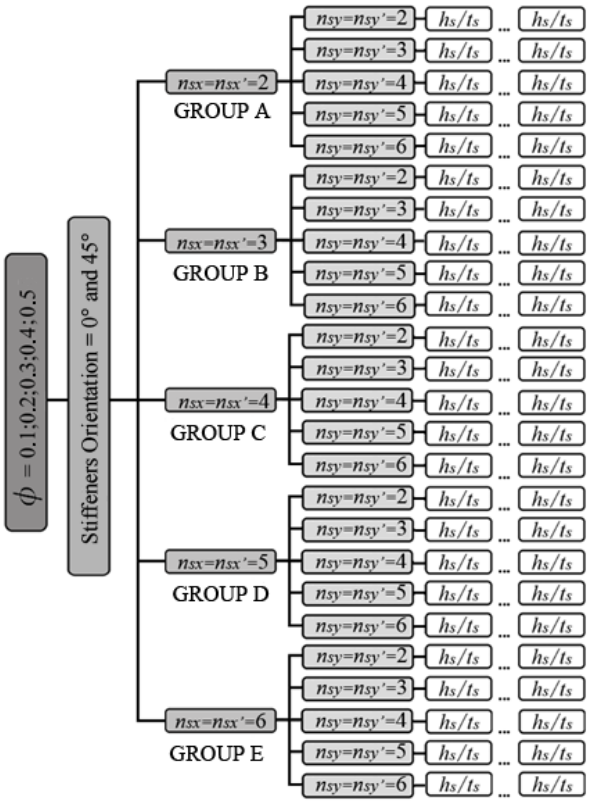

Figure 6. Application of the CDM in the definition of the search space.

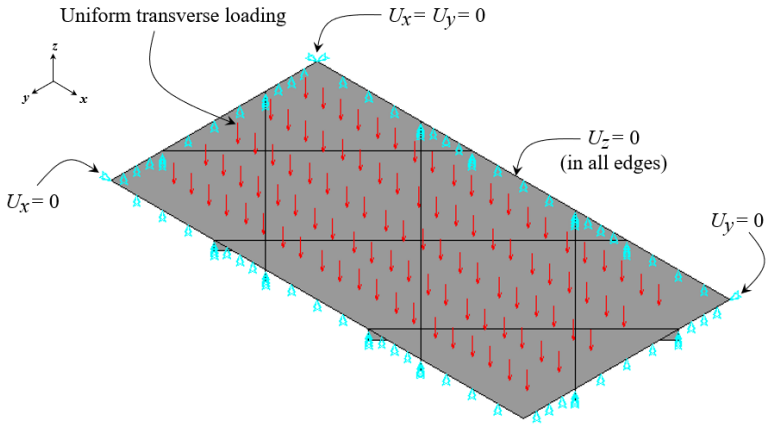

Figure 7. Plate P'(3,3): Boundary conditions and loading.

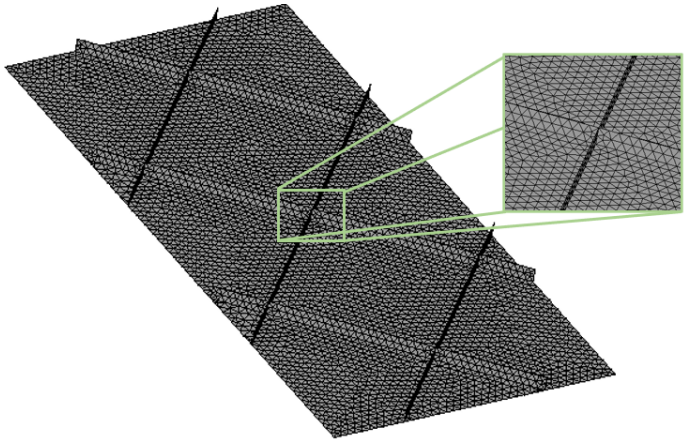

Figure 8. Plate P'(3,3): Discretized model.

2.3. Geometric Optimization

From the definition of the search space (see Fig. 6), the Exhaustive Search (ES) technique was used to compare the mechanical behavior of all proposed geometric configurations. The optimum geometry is one that minimizes the maximum deflection of the stiffened plates.

In summary, the methodology adopted in this work is showed in Fig. 9.

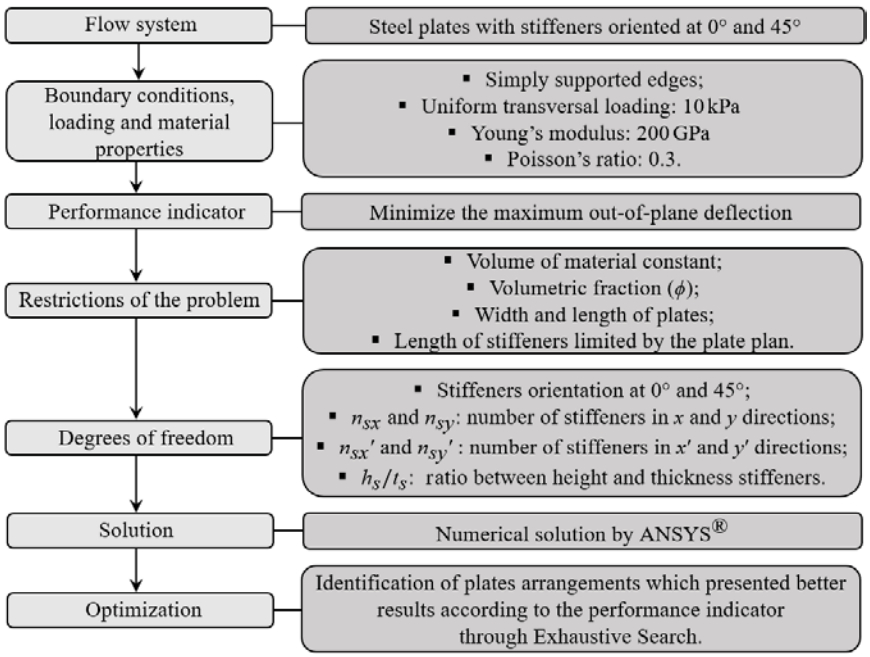

Figure 9. Geometrical optimization methodology.

3. Results and Discussion

Initially, a mesh convergence test was carried out in order to determine the appropriate size of finite elements that would compose the meshes of the cases to be numerically simulated. For this purpose, it was adopted the most complex geometry of the search space: the plate P'(6,6) with a volumetric fraction ϕ = 0.5 and higher ratio h_s/t_s = 38.664. The size of the finite elements has been reduced successively, taking as reference the width of the plate *b* = 1000 mm, following to the criterion established by Troina et al. [15]. The result can be observed in Fig. 10.

As can be seen in Fig. 10, from the mesh M_3 with finite element size of 16.67 mm, there was a convergence of values for the maximum deflection U_zMax, so that this is the finite element size stated to discretize the meshes of all computational domains.

The variation of the maximum deflection according to the variation of ratio h_s/t_s, for all proposed plates, is presented in Figs. 11 to 35. Observing these results, it was possible to attest that transforming a portion of material from the non-stiffened reference plate, maintaining the total material volume constant, as predetermined by the CDM, improvements of the mechanical behavior regarding the maximum deflection U_zMax can be reached, since all maximum deflections found for the stiffened plates are smaller than the U_zMax = 0.697 mm, obtained for the reference plate. This behavior is in agreement with Troina et al. [15] for plates with stiffeners oriented at 0°, being also observed for plates with stiffeners oriented at 45°. For instance, comparing the plate P'(6,5) with h_s/t_s = 58.778 and U_zMax = 0.0174 mm, referring to ϕ = 0.4, which presented the lowest maximum deflection among the places with stiffeners at 45°, with the reference plate, the reduction of maximum deflection was 97.50 %. In its turn, comparing the reference plate with the worst result for plates with stiffeners at 45 °, obtained by the plate P'(2,2) with h_s/t_s = 22.019 and U_zMax = 0.2134 mm for ϕ = 0.5, there was a reduction of 69.30 % in maximum deflection.

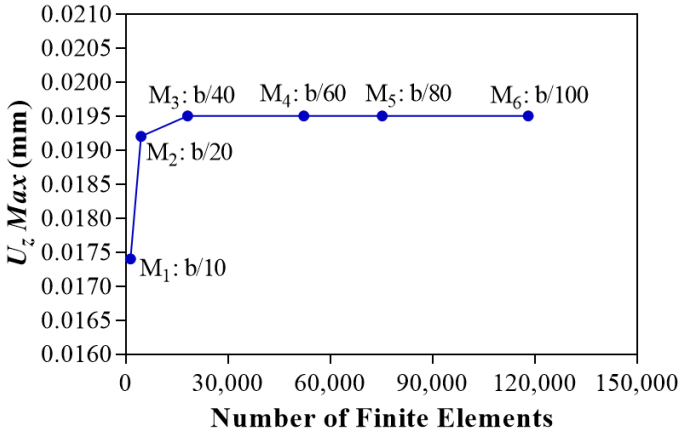

Figure 10. Mesh convergence test.

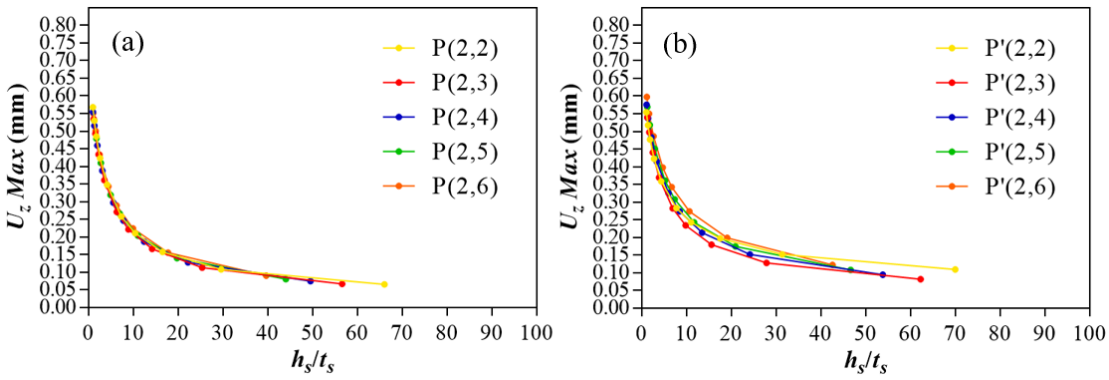

Figure 11. ϕ = 0.1 - Group A: (a) stiffeners at 0 °; (b) stiffeners at 45 °.

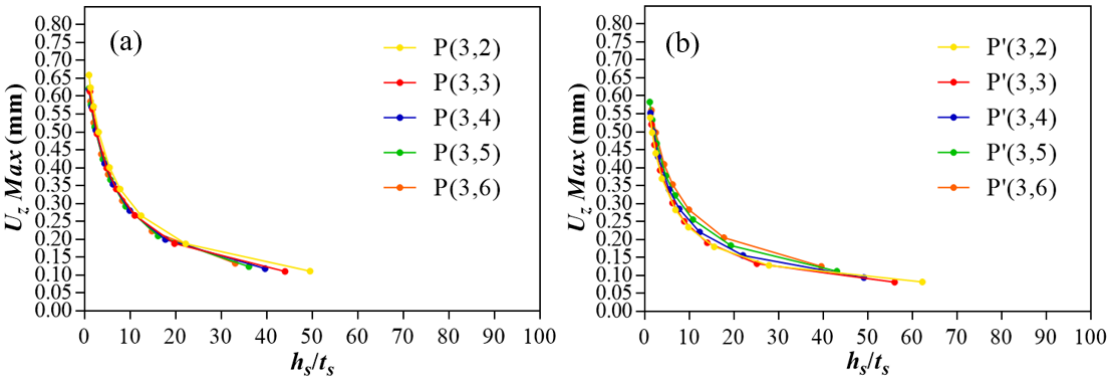

Figure 12. ϕ = 0.1 - Group B: (a) stiffeners at 0 °; (b) stiffeners at 45 °.

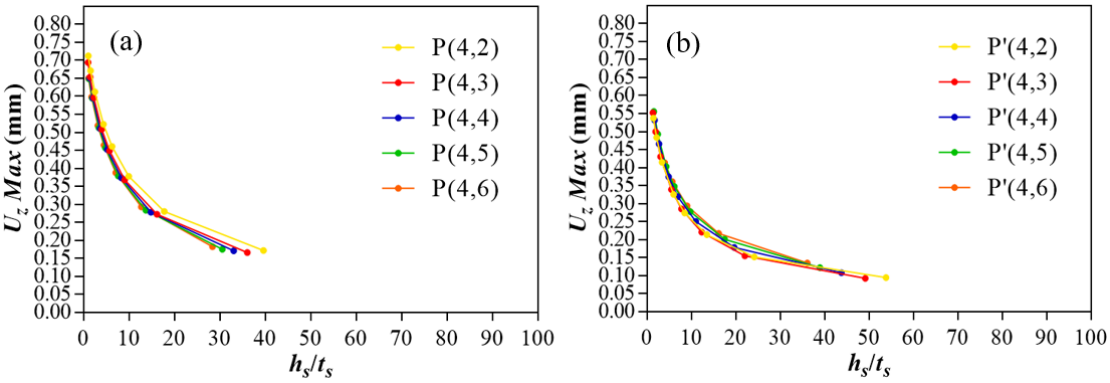

Figure 13. ϕ = 0.1 - Group C: (a) stiffeners at 0 °; (b) stiffeners at 45 °.

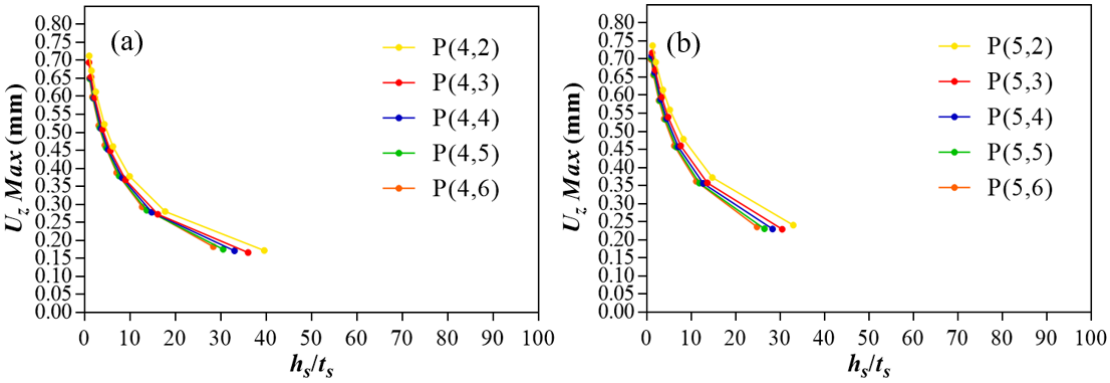

Figure 14. ϕ = 0.1 - Group D: (a) stiffeners at 0 °; (b) stiffeners at 45 °.

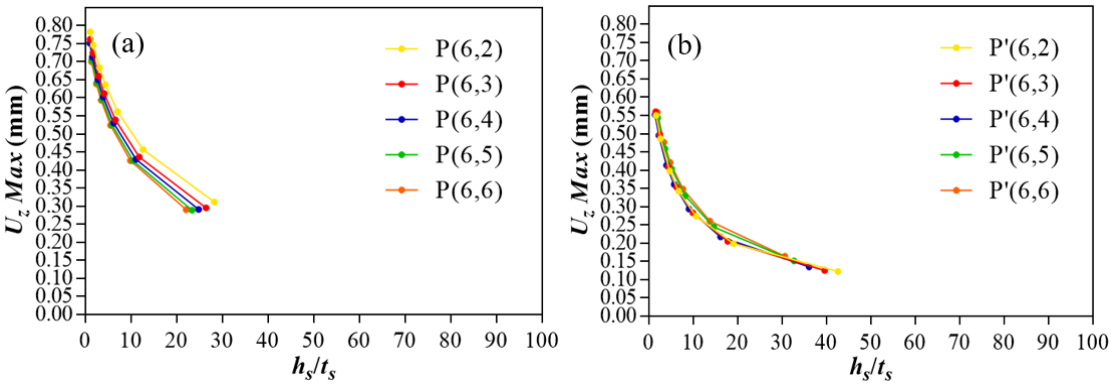

Figure 15. ϕ = 0.1 - Group E: (a) stiffeners at 0 °; (b) stiffeners at 45 °.

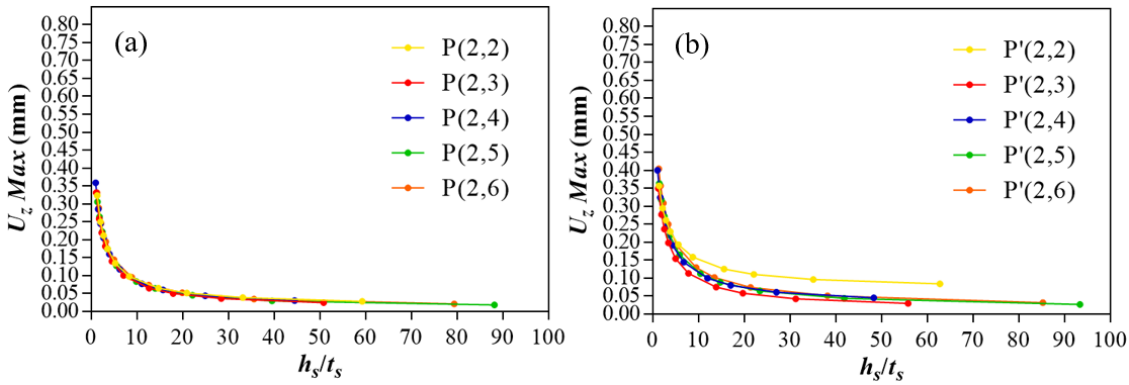

Figure 16. ϕ = 0.2 - Group A: (a) stiffeners at 0 °; (b) stiffeners at 45 °.

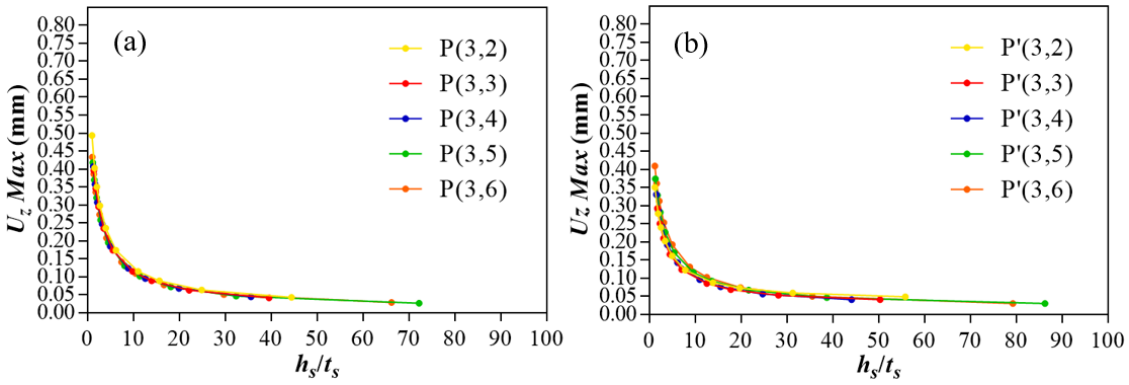

Figure 17. ϕ = 0.2 - Group B: (a) stiffeners at 0 °; (b) stiffeners at 45 °.

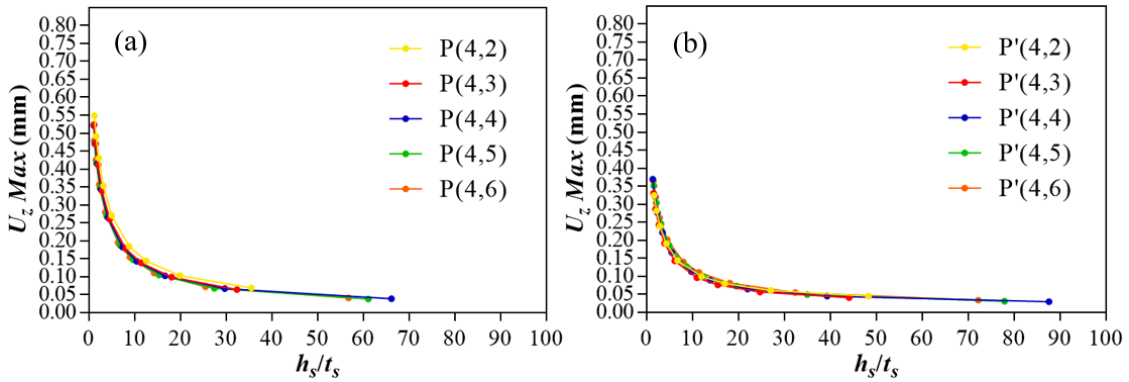

Figure 18. ϕ = 0.2 - Group C: (a) stiffeners at 0 °; (b) stiffeners at 45 °.

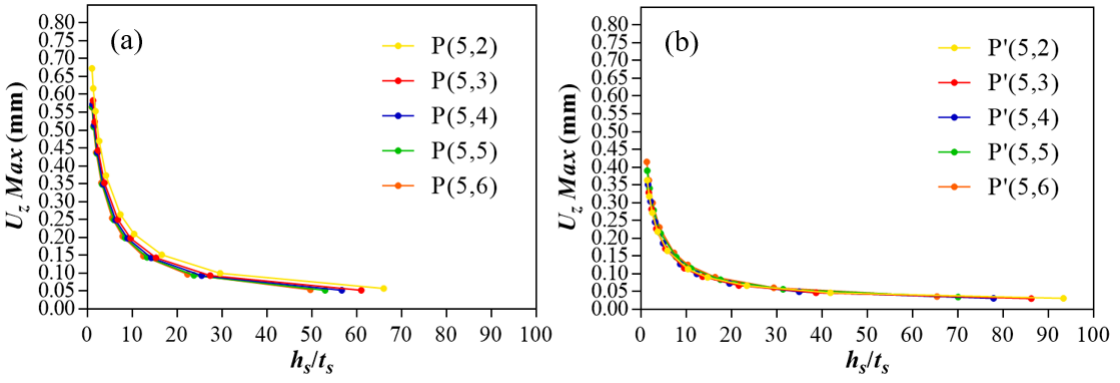

Figure 19. ϕ = 0.2 - Group D: (a) stiffeners at 0 °; (b) stiffeners at 45 °.

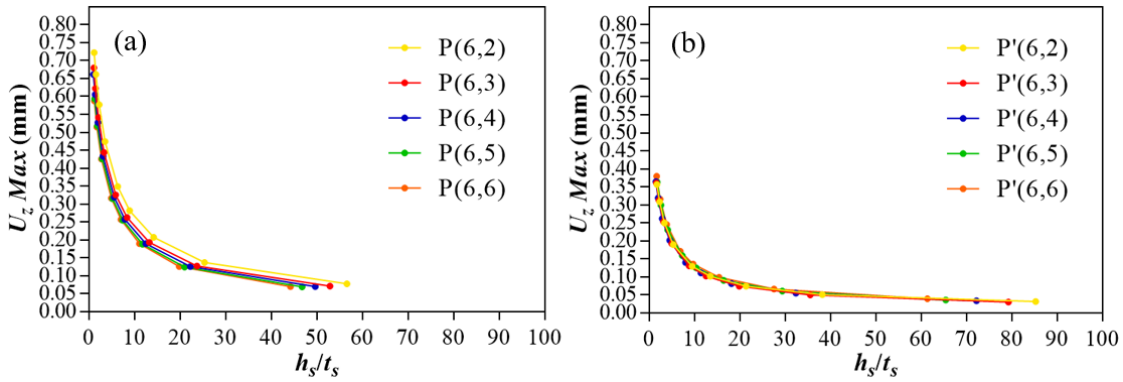

Figure 20. ϕ = 0.2 - Group E: (a) stiffeners at 0 °; (b) stiffeners at 45 °.

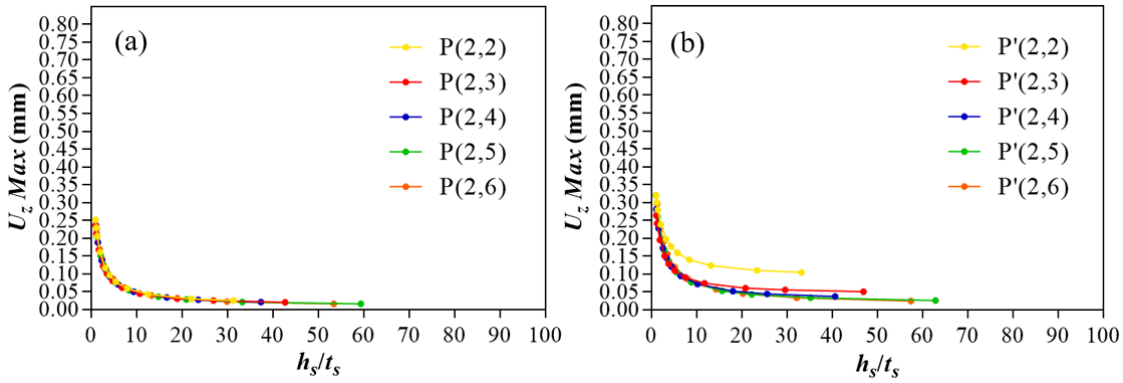

Figure 21. ϕ = 0.3 - Group A: (a) stiffeners at 0 °; (b) stiffeners at 45 °.

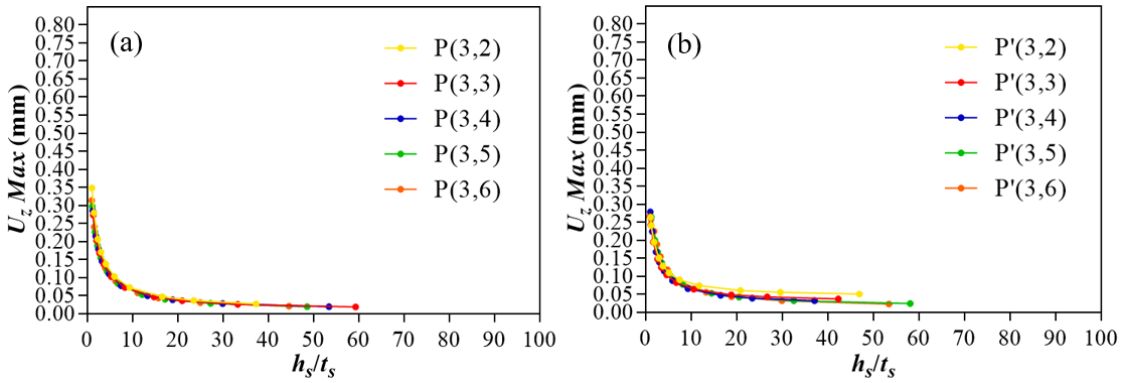

Figure 22. ϕ = 0.3 - Group B: (a) stiffeners at 0 °; (b) stiffeners at 45 °.

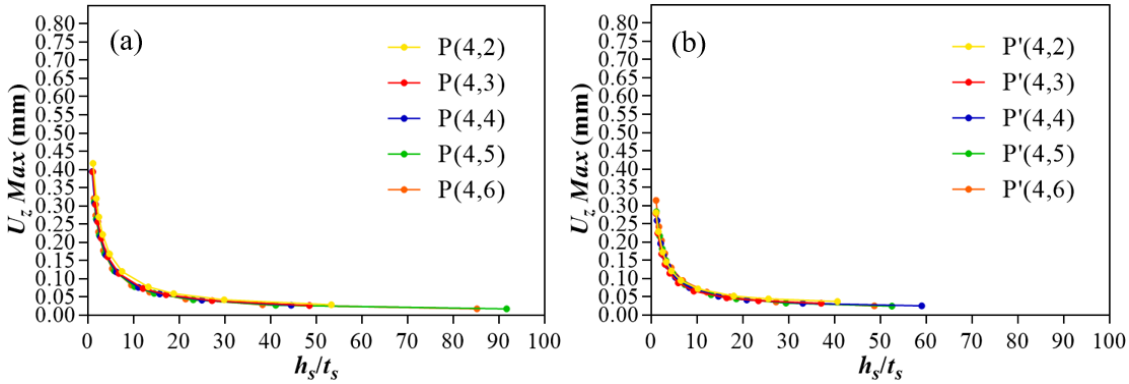

Figure 23. ϕ = 0.3 - Group C: (a) stiffeners at 0 °; (b) stiffeners at 45 °.

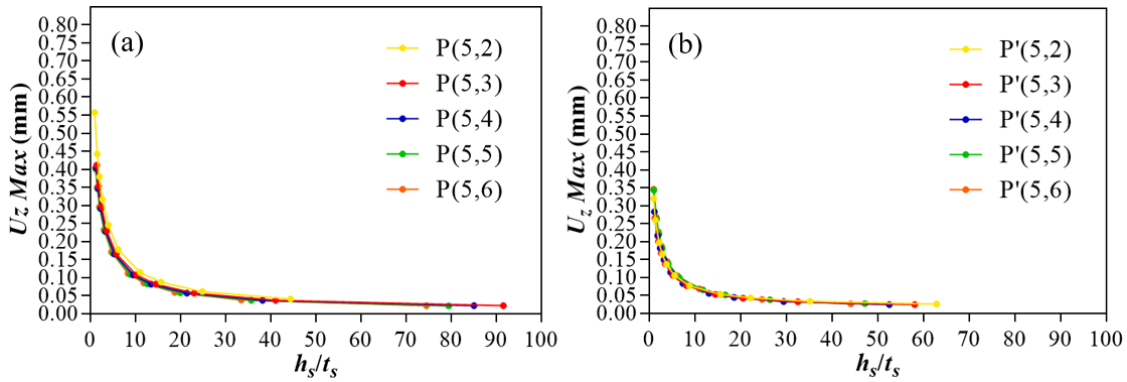

Figure 24. ϕ = 0.3 - Group D: (a) stiffeners at 0 °; (b) stiffeners at 45 °.

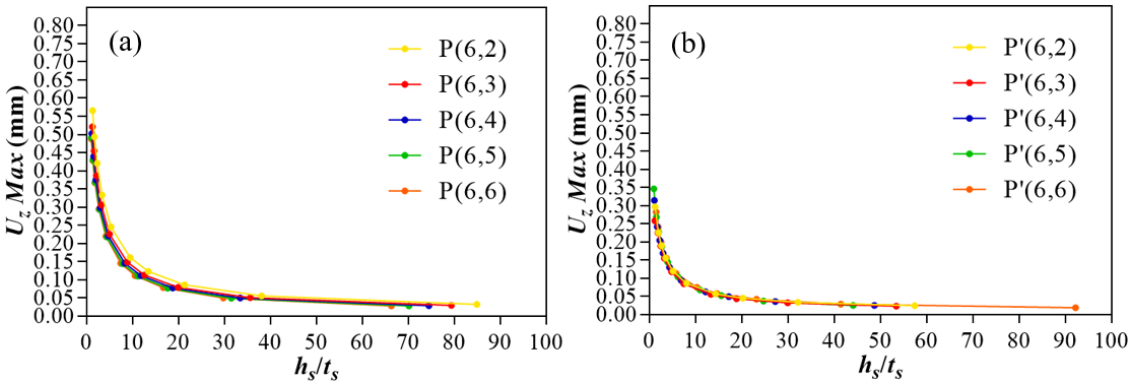

Figure 25. ϕ = 0.3 - Group A: (a) stiffeners at 0 °; (b) stiffeners at 45 °.

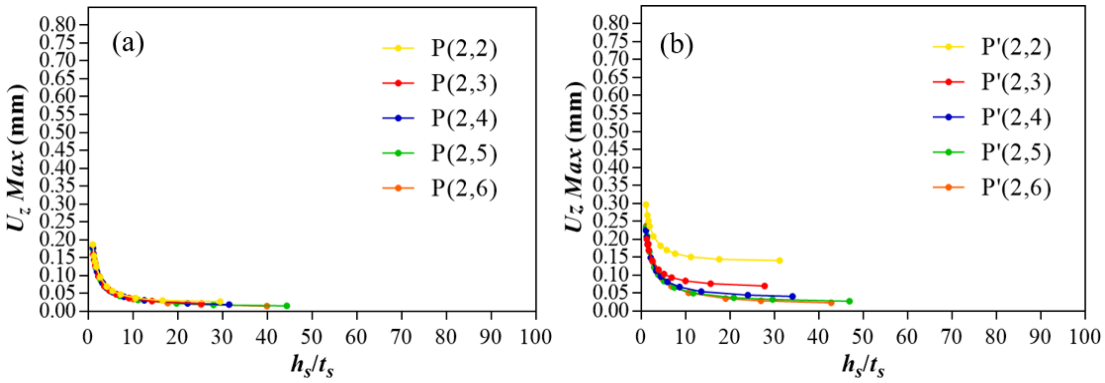

Figure 26. ϕ = 0.4 Group A: (a) stiffeners at 0 °; (b) stiffeners at 45 °.

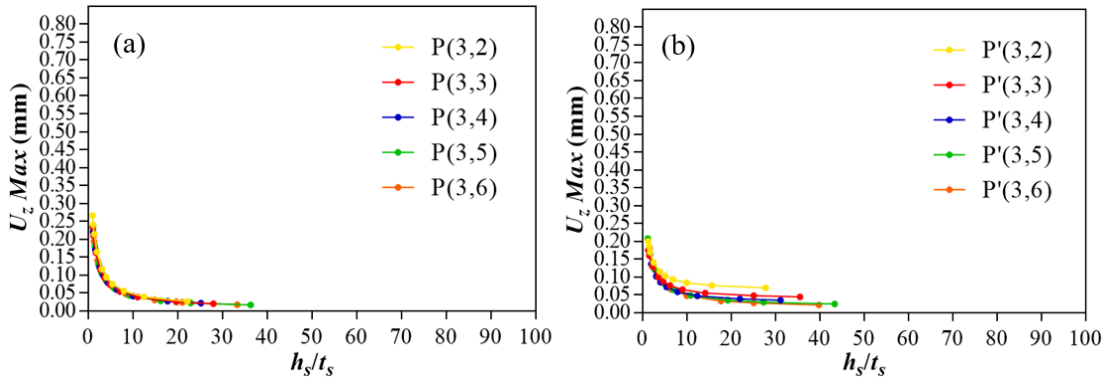

Figure 27. ϕ = 0.4 - Group B: (a) stiffeners at 0 °; (b) stiffeners at 45 °.

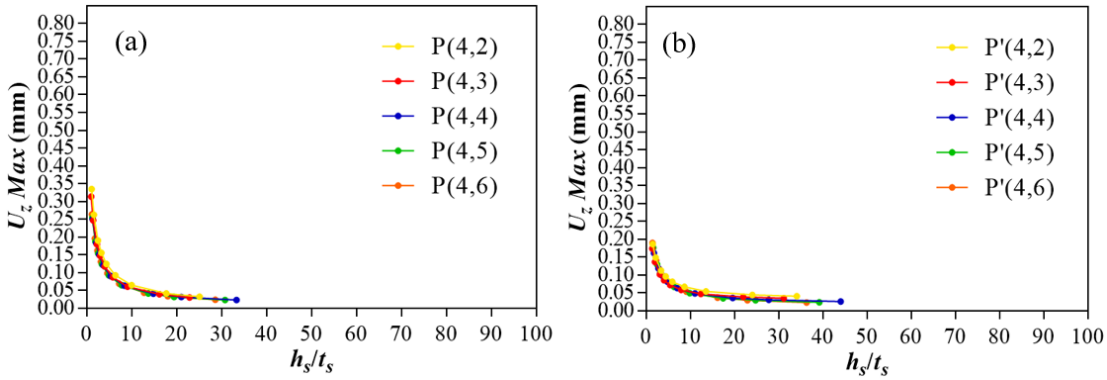

Figure 28. ϕ = 0.4 - Group C: (a) stiffeners at 0 °; (b) stiffeners at 45 °.

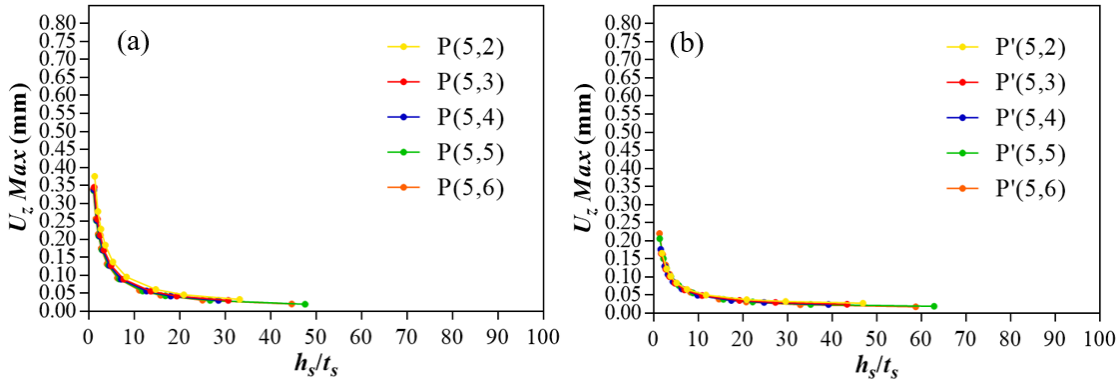

Figure 29. ϕ = 0.4 - Group D: (a) stiffeners at 0 °; (b) stiffeners at 45 °.

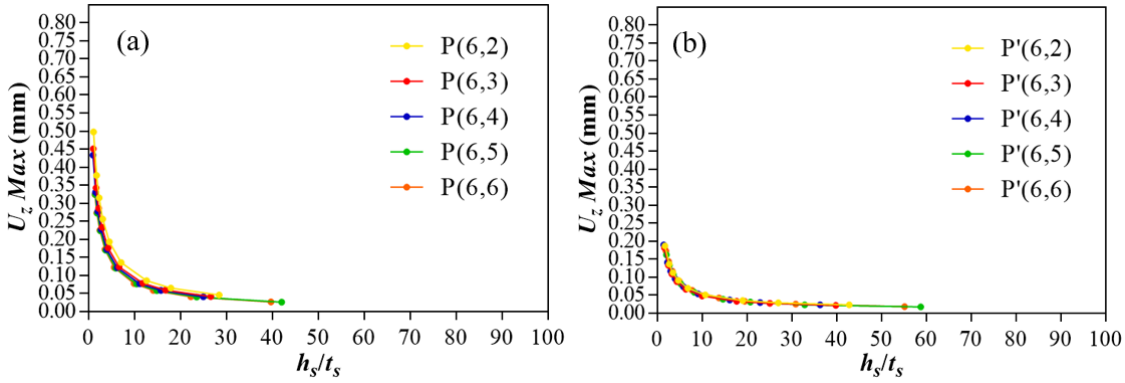

Figure 30. ϕ = 0.4 - Group E: (a) stiffeners at 0 °; (b) stiffeners at 45 °.

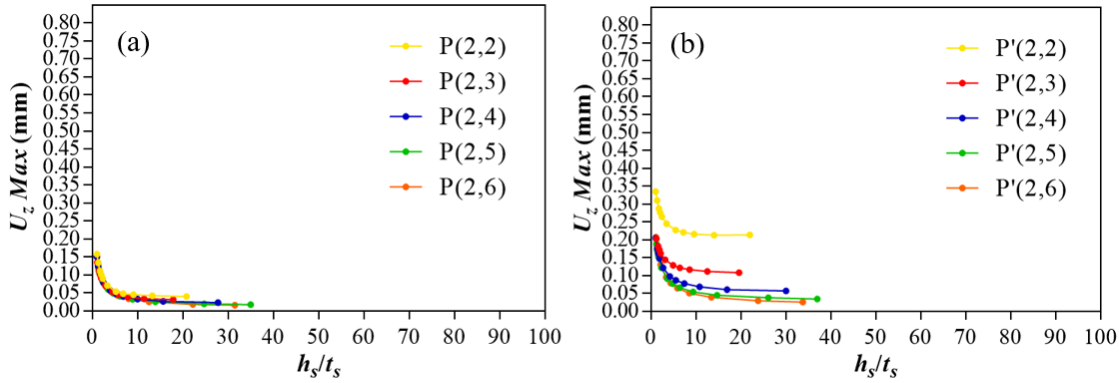

Figure 31. ϕ = 0.5 - Group A: (a) stiffeners at 0 °; (b) stiffeners at 45 °.

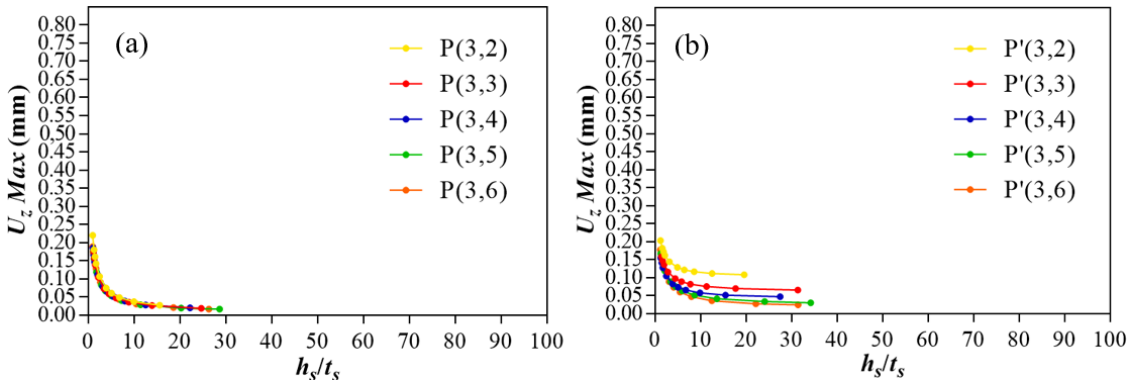

Figure 32. ϕ = 0.5 - Group B: (a) stiffeners at 0 °; (b) stiffeners at 45 °.

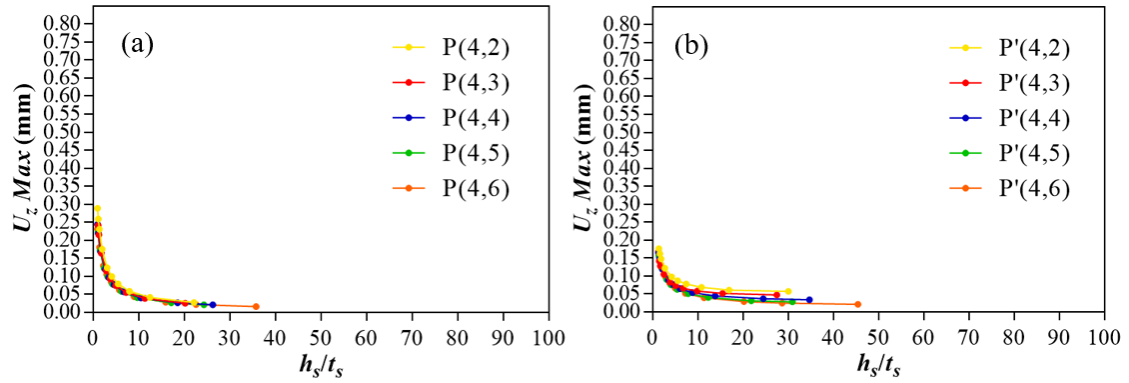

Figure 33. ϕ = 0.5 - Group C: (a) stiffeners at 0 °; (b) stiffeners at 45 °.

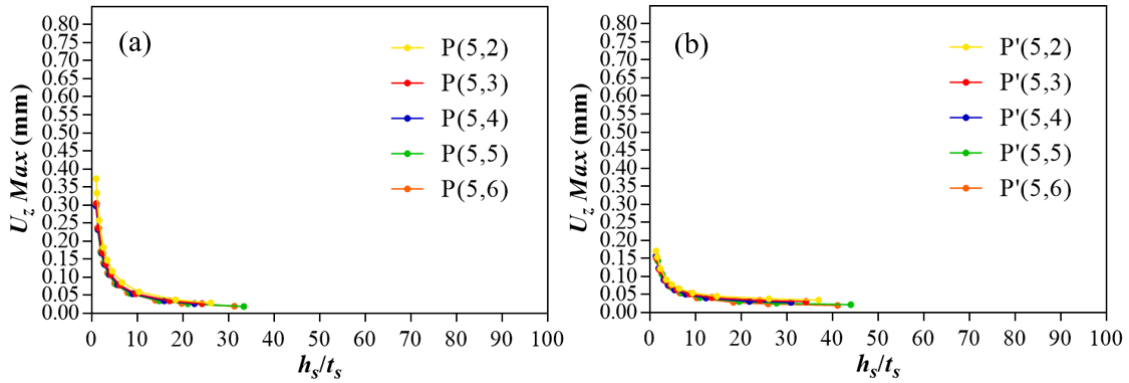

Figure 34. ϕ = 0.5 - Group D: (a) stiffeners at 0 °; (b) stiffeners at 45 °.

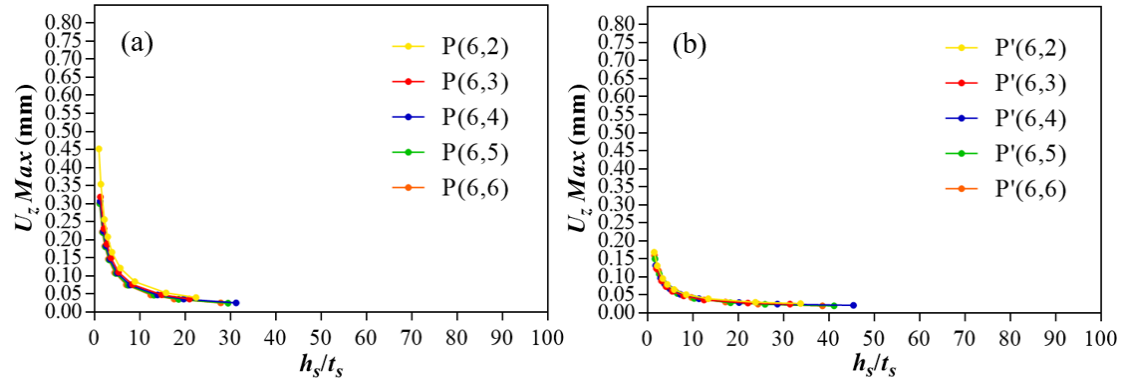

Figure 35. ϕ = 0.5- Group E: (a) stiffeners at 0 °; (b) stiffeners at 45 °.

Then, from the Figs. 11 to 35, the results for the stiffened plates that achieved the lowest maximum deflections are presented in bar graphs, considering the two stiffeners orientations (0 ° and 45 °), for each ϕ value (0.1 to 0.5), following the group division previously established (see Fig. 6). These results are shown in Figs. 36 to 40, respectively, for ϕ = 0.1 to 0.5.

It is worth to emphasize that the comparison of the results was performed between equivalent plates, i.e., with the same ϕ value, thickness and amounts of stiffeners in the *x*-*x*' and *y*-*y*' directions, being the stiffeners orientation the only differential. Thereby, it was possible to observe the direct influence of this degree of freedom on the stiffened plates behavior.

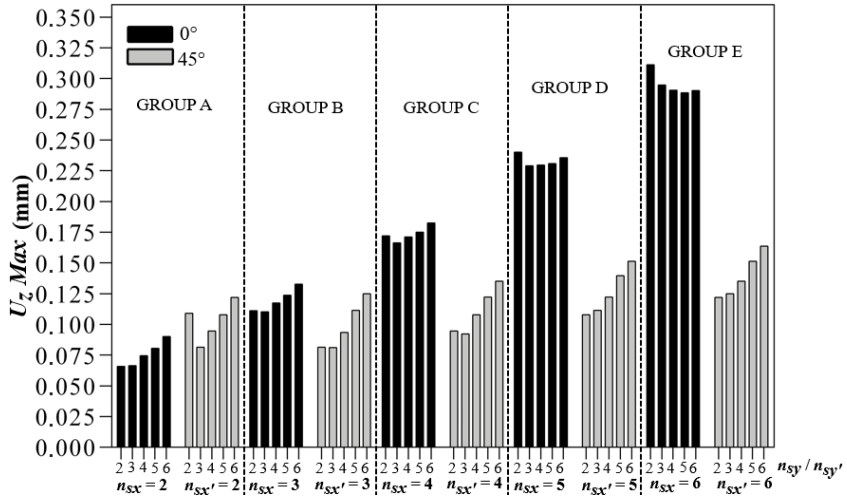

Figure 36. Results for ϕ = 0.1.

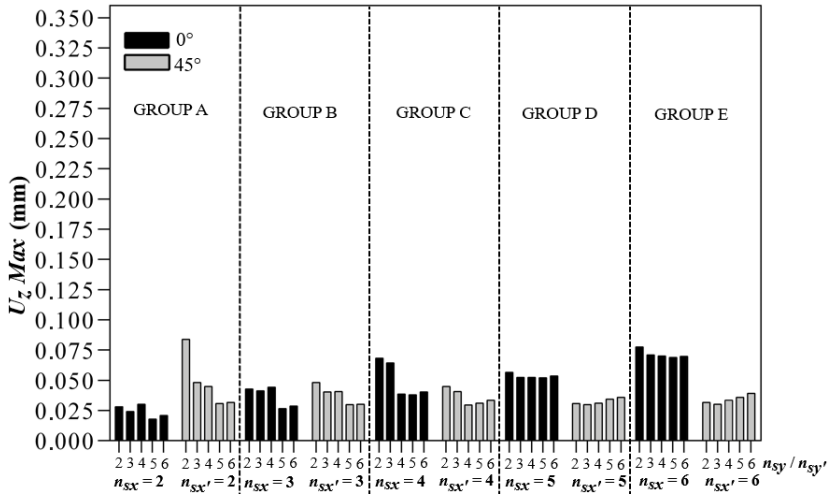

Figure 37. Results for ϕ = 0.2.

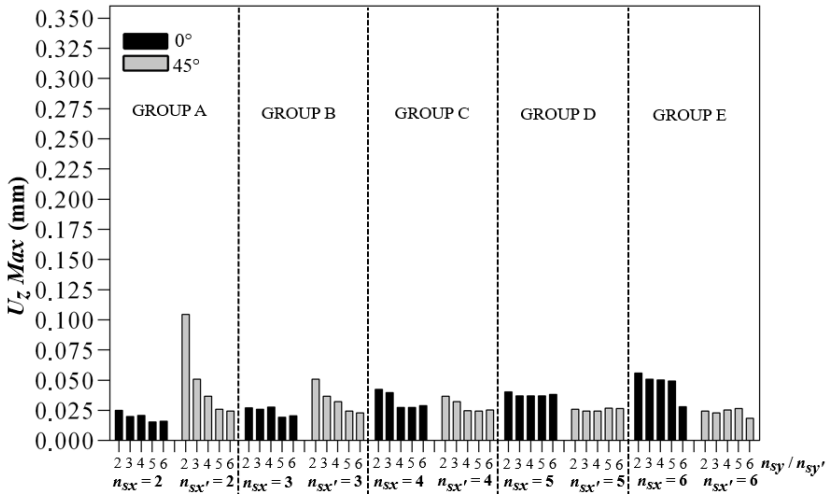

Figure 38. Results for ϕ = 0.3.

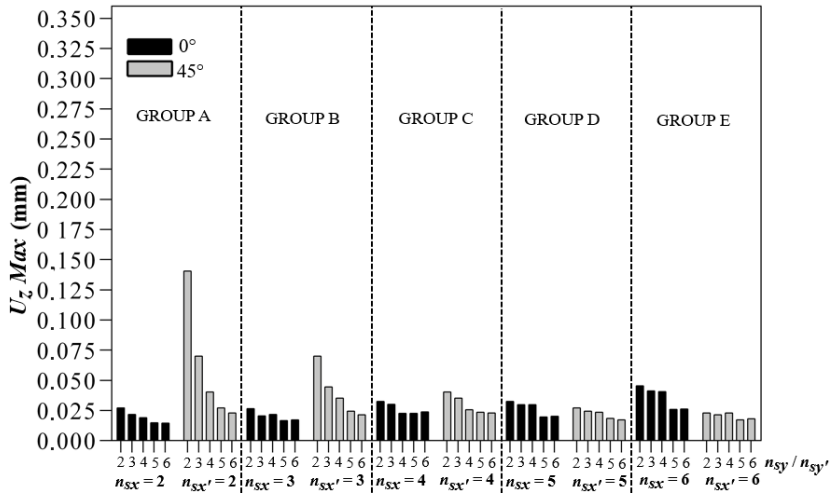

Figure 39. Results for ϕ = 0.4.

Observing the results of ϕ = 0.1 (Fig. 36), one can note that, excepting Group A, the plates with stiffeners oriented at 45 ° showed lower deflections than the plates with stiffeners oriented at 0 °. Taking the Group B as reference, the plate that reached the lowest maximum deflection was P'(3,3) with h_s/t_s = 56.091 and U_{zMax} = 0.0811 mm, presents a reduction of 26.50 % in comparison to the plate P(3,3) with h_s/t_s = 44.090, which registered U_zMax = 0.1103 mm. In turn, with respect to percentage differences, the largest one occurred between the plates P'(6,2) with h_s/t_s = 42.650 which presented U_{zMax} = 0.1220 mm and P(6,2) with h_s/t_s = 28.331 and U_zMax = 0.3113 mm, meaning a reduction of 60.81 % in favor of the plate with stiffeners oriented at 45 °.

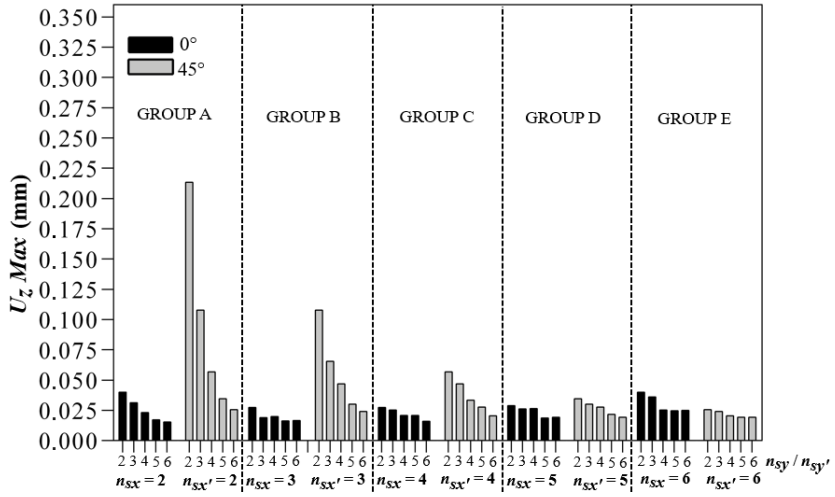

Figure 40. Results for ϕ = 0.5.

Regarding to the volumetric fraction ϕ = 0.2 (Fig. 37), it was noted that in a general way the maximum deflections tend to be smaller compared to values of ϕ = 0.1 (see Fig. 36). This is justified by the fact that a greater amount of material was destined to design of the stiffeners. It was also noted that the plates with stiffeners oriented at 45 ° become more advantageous as from Group C; standing out the plate P'(4,4) with h_s/t_s = 87.652 that presented the lowest maximum deflection U_zMax = 0.0297 mm, a minimization of 22.98 % compared to the plate P(4,4) with h_s/t_s = 66.206, which showed U_zMax = 0.0385 mm. However, the widest percentage reduction in maximum deflection favorable to the plate with stiffeners at 45 °, it was presented by the plate P'(6,2) and h_s/t_s = 85.301 with U_zMax = 0.0316 mm, achieving a value 59.2 % lower than the U_zMax = 0.0775 mm of the plate P(6,2) with h_s/t_s = 56.662.

Concerning Fig. 38, which presents the results for ϕ = 0.3, it was perceptible a similar behavior to ϕ = 0.2 (see Fig. 37). In other words, from Group C all plates with stiffeners oriented at 45 ° have smaller maximum deflections in comparison to the plates with stiffeners oriented at 0 °. In relation to the best result for plates with stiffeners at 45 ° for ϕ = 0.3, the plate P'(6,6) with h_s/t_s = 92.275 achieved

U_zMax = 0.0186 mm, i.e., a maximum deflection 33.84 % smaller than the plate P(6,6) with h_s/t_s = 66.348 which reached U_zMax = 0.0282 mm. For illustration purposes, this reduction in the maximum deflection can be seen in Fig. 41. However, the biggest percentage difference happened between the plates P'(6,2) with h_s/t_s = 57.464 which registered U_zMax = 0.0245 mm and P(6,2) with h_s/t_s = 38.145 which presented U_zMax = 0.0559 mm, reaching a minimization of 56.10 % favorable to the plate with stiffeners at 45 °.

In its turn, for ϕ = 0.4 the Fig. 39 indicates that the mechanical behavior of the stiffened plates with stiffeners at 45 ° is majoritarily superior only in Groups D and E. The best result for the plate with stiffeners at 45 ° was to P'(6,5) with h_s/t_s = 58.778 and U_zMax = 0.0174 mm, representing a minimization of 32.96 % in the maximum deflection comparing to the P(6,5) plate with h_s/t_s = 42.067 and U_zMax = 0.0259 mm. Nevertheless, the larger achieved reduction in maximum deflection it was 47.78 % comparing the plate P'(6,2) with h_s/t_s = 42.873 and U_zMax = 0.0229 mm with the plate P(6,2) with h_s/t_s = 28.498 which presented U_zMax = 0.0454 mm.

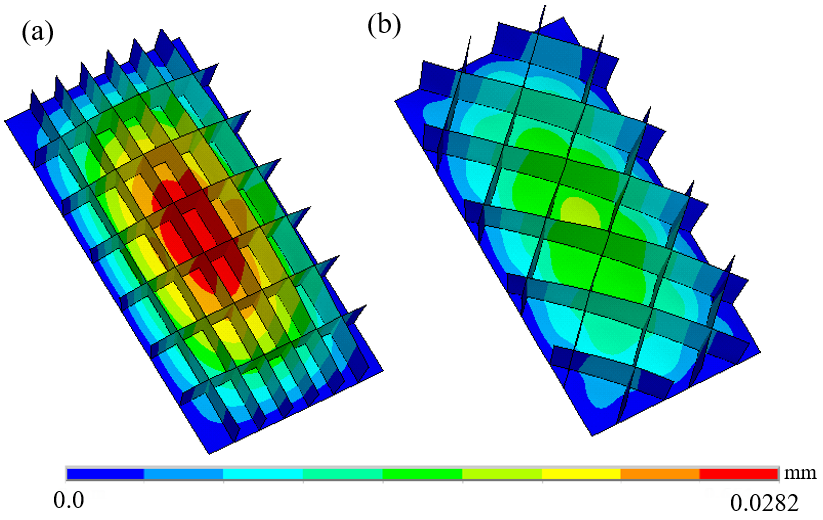

Figure 41. Deflection distribution: (a) P(4,5); (b) P'(4,5).

Finally, dealing with the volumetric fraction ϕ = 0.5 (Fig. 40), it was observed that the plates with stiffeners oriented at 45 ° have a superior mechanical behavior predominant only in Group E. For instance, the plate P'(6,5) with h_s/t_s = 41.177 and U_zMax = 0.0194 mm, that showed the lowest maximum deflection, achieved a reduction of 21.40 % in relation to the plate P(6,5) with h_s/t_s = 29.507 and U_zMax = 0.0247 mm. In addition, the largest percentage difference occurred when comparing the plate P'(6,2) with h_s/t_s = 33.801 and U_zMax = 0.0256 mm, which presented a reduction in the maximum deflection of 36.12 %, and the plate P(6,2) with h_s/t_s = 22.476 and U_zMax = 0.0401 mm.

Still observing Fig. 40, it was possible to notice an accentuated maximum deflection presented by the plate with stiffeners oriented at 45° P'(2,2), being observed this same behavior for the other ϕ values. This is due to the equidistant distribution of the stiffeners, which for the plates with stiffeners at 45 ° it was performed as a relation of the diagonals; while for the plates with stiffeners at 0 ° it was generated as a relation of the orthogonal edges. Hence, the plate P'(2,2) has a non-stiffened central area larger than the central area of plate P(2,2), concentrating the deflection field in this region, as shown in Fig. 42.

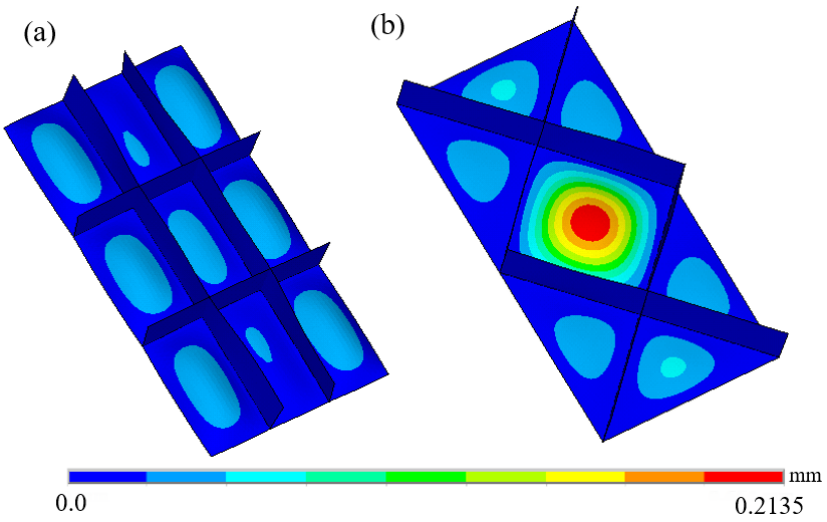

Figure 42. Deflection distribution: (a) P(2,2); (b) P'(2,2).

Analyzing Fig. 36 to 40, one can observe a tendency: as the volumetric fraction ϕ increases, the plates with stiffeners oriented at 45 ° began to show better mechanical behavior only for plates with larger amounts of stiffeners. When ϕ = 0.1 (Fig. 36) plates with stiffeners at 45 ° are the best for the Groups B, C, D and E; when ϕ = 0.2 (Fig. 37) and ϕ = 0.3 (Fig. 38) for the Groups C, D and E; when ϕ = 0.4 (Fig. 39) for the Groups D and E; and when ϕ = 0.5 (see Fig. 40) just for Group E. This trend can be better observed in Fig. 43, where the best results per group were plotted for each volumetric fraction ϕ.

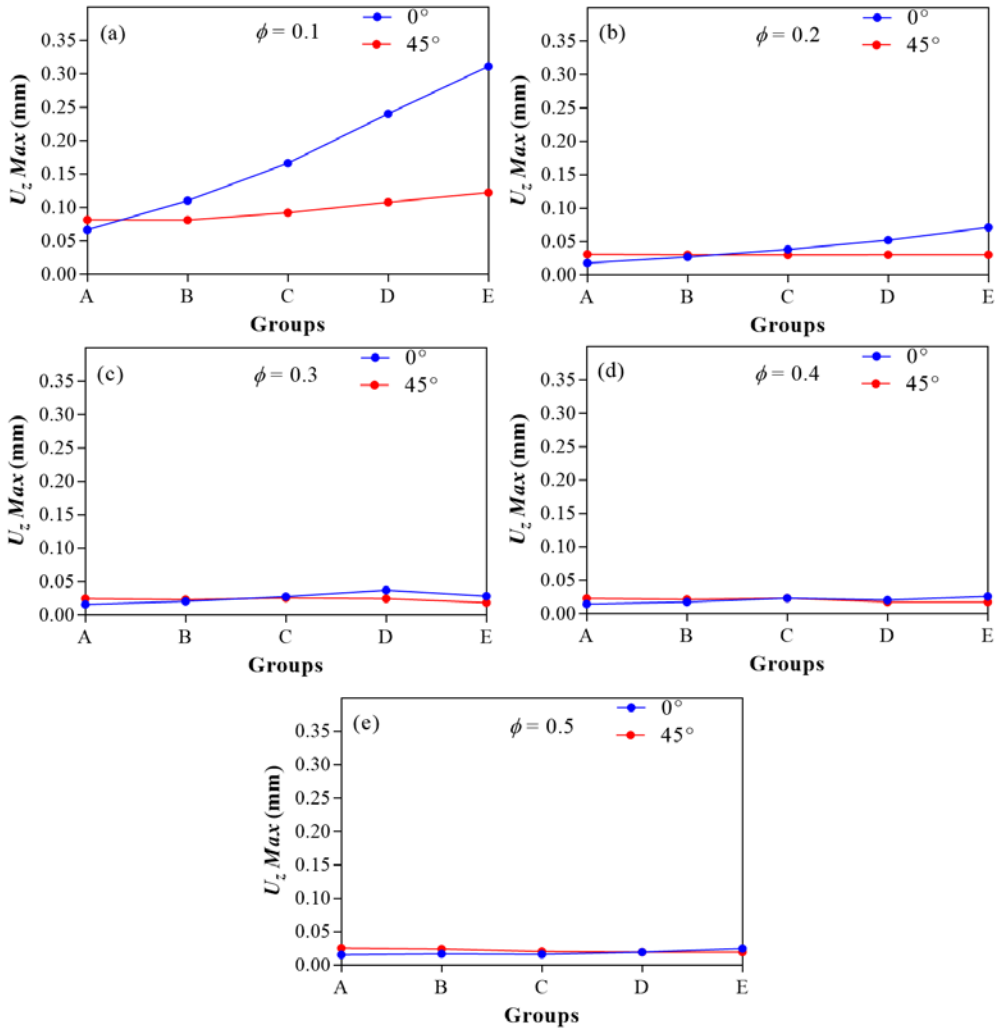

Figure 43. Best results per group: (a) ϕ = 0.1; (b) ϕ = 0.2; (c) ϕ = 0.3; (d) ϕ = 0.4; and (d) ϕ = 0.5.

Fig. 44 presents the optimized results for each volumetric fraction ϕ considering just the groups A and E, i.e., the groups with the smallest and largest quantities of stiffeners, respectively. That way it was possible to observe which was previously stated, that plates with stiffeners oriented at 45 ° are more advantageous for large amounts of stiffeners.

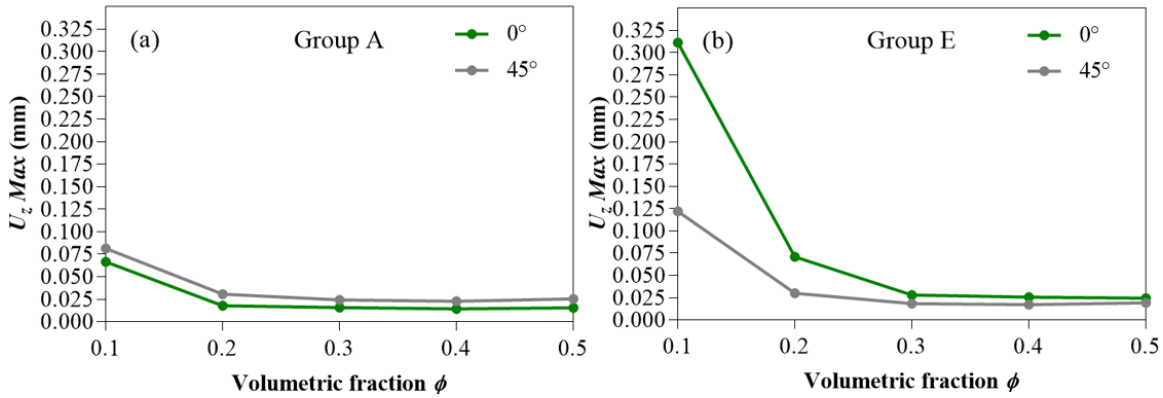

Figure 44. Optimized results: (a) Group A; (b) Group E.

Finally, Fig. 45 presents the maximum von Mises stress for the same stiffened plates of Fig. 44. The main purpose here is to show the stress level achieved by the studied structures through this representative sampling.

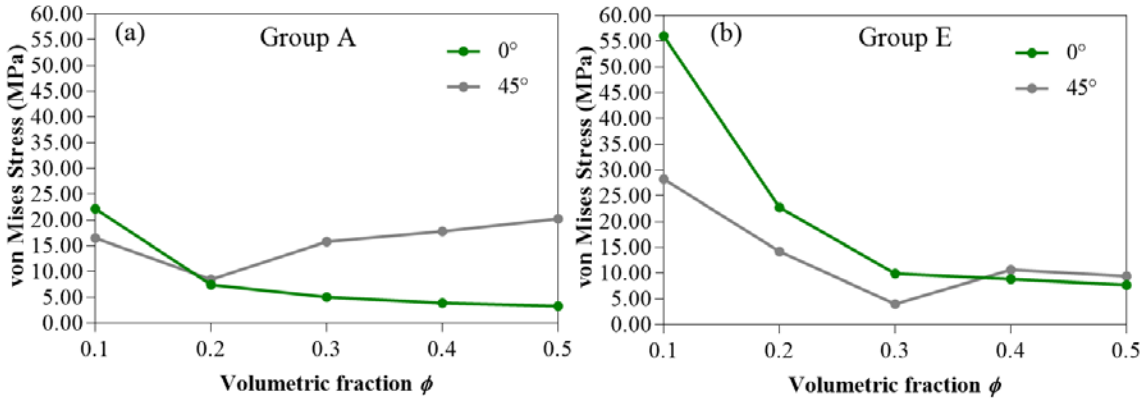

Figure 45. Maximum von Misses stress for the stiffened plates of Fig. 44.

From Fig. 45 one can note that the magnitude reached by the von Mises stress is considerably smaller than the steel yielding stress (250 MPa). For instance, the minimum factor of safety related to the steel yielding stress is around 4.5, obtained by the worst case, i.e., the one that achieved the maximum von Mises stress value (ϕ = 0.1, stiffeners oriented at 45 ° and Group E, in Fig. 45b).

Therefore, due to the low load magnitude of 10 kPa adopted for all cases, it is possible to affirm that the linear-elastic behavior adopted for the steel is an adequate approach. From this, the optimum geometric configurations obtained for the minimization of the maximum deflection can be used with higher values for the uniform transverse load, since the stress limit be not reached.

Another important aspect that emerged from Fig. 45 is that the optimized geometry defined when the maximum deflection is the performance parameter, as proposed in the present work, is not necessarily the same if the parameter performance is changed for the maximum von Mises stress.

4. Conclusion

Applying CDM, FEM and ES technique, it was possible to evaluate the behavior of different stiffened plate arrangements regarding the maximum deflection considering the stiffeners oriented at 0 ° and 45 °, aiming their geometric optimization.

Firstly, it was concluded that keeping constant the total material volume of a non-stiffened steel plate and transforming a portion of its material (fully deducted from the thickness) into stiffeners, it was possible to significantly improve the mechanical behavior, achieving reductions in the maximum deflection around 95 %. In addition, as already expected, it was observed that the variation of the h_s/t_s ratio causes a relevant influence on the rigidity of the plates, for both stiffeners oriented at 0° and stiffeners oriented at 45 °.

For most of the analyzed plate arrangements, orienting the stiffeners at 45 ° is more advantageous to reduce the maximum deflection compared to the plates with stiffeners oriented at 0 °, mainly for the values of ϕ = 0.1, 0.2 and 0.3, where it was possible to minimize the maximum deflection in the order of 60 % in some arrangements with stiffeners at 45°. The results also showed that, for larger percentages of material transformed into stiffeners (ϕ = 0.4 and 0.5), orienting stiffeners at 45 ° becomes viable for larger amounts of stiffeners.

It is important to emphasize that applying the ES technique on the search space, the optimal geometry that showed the lowest maximum deflection for plates with stiffeners at 45° was the plate P'(6,5) with h_s/t_s = 58.778 (having h_s = 279.193 mm and t_s = 4.75 mm) relative to ϕ = 0.4 (i.e. t_p = 12 mm), which showed U_zMax = 0.0174 mm.

In future works, it would be interesting to investigate other values of ϕ, as well as, other stiffeners orientations concerning the minimization of the maximum deflections and/or the maximum von Mises stress.

5. Acknowledgement

This work was performed with the support of the: *Coordenação de Aperfeiçoamento de Pessoal de Nível Superior – Brasil* (CAPES) – Finance Code 001, *Fundação de Amparo à Pesquisa do Estado do Rio Grande do Sul – Brasil* (FAPERGS) and *Conselho Nacional de Desenvolvimento Científico e Tecnológico – Brasil* (CNPq). Particularly, the authors L.A.O. Rocha, E.D. dos Santos and L.A. Isoldi thank to CNPq for their research grants (Processes: 307791/2019-0, 306024/2017-9 and 306012/2017-0, respectively).

References

1. Ventsel, E., Krauthammer, T. Thin Plates and Shells: Theory, Analysis and Applications. 1ª ed. Marcel Dekker: New York, 2001. DOI: 10.1201/9780203908723
2. Reddy, J.N. Theory and Analysis of Elastic Plates and Shells. 2ª ed., Boca Raton: CRC Press, 2007.
3. Szilard, R. Theories and applications of plate analysis: Classical numerical and engineering methods. 1ª ed., Wiley: Hoboken, 2004. DOI: 10.1002/97804701728722
4. Bedair, O.K. Analysis and Limit State Design of stiffened plates and shells: A world view. Applied Mechanics Reviews. 2009. 62(2). Pp. 01–16. DOI: 10.1115/1.3077137
5. Tyukalov, Yu. Calculation method of bending plates with assuming shear deformations. Magazine of Civil Engineering. 2019. 85(1). Pp. 107–122. DOI: 10.18720/MCE.85.9
6. Tyukalov, Yu. Finite element model of Reisner's plates in stresses. Magazine of Civil Engineering. 2019. 89(5). Pp. 61–78. DOI: 10.18720/MCE.89.6
7. Powell, G.H., Ogden, D.W. Analysis of orthotropic steel plate bridge decks. Journal of the Structural Division. 1969. 95. Pp. 909–921.
8. Rossow, M.P., Ibrahimkhail, A.K. Constraint method analysis of stiffened plates. Computers and Structures. 1978. 8(1). Pp. 51–60.
9. Mukhopadhyay, M., Satsangi, S.K. Isoparametric stiffened plate bending element for the analysis of ship's structure. Royal Institution of Naval Architects Transactions. 1984. 126. Pp. 141–151.
10. Kukreti, A.R., Cheraghi, E. Analysis procedure for stiffened plate systems using an energy approach. Computers & Structures. 1993. 46(4). Pp. 649–657.
11. Bedair, O.K. Analysis of stiffened plates under lateral loading using sequential quadratic programming (SQP). Computers & Structures. 1997. 62(1). Pp. 63–80. DOI: 10.1016/S0045-7949(96)00281-7
12. Tanaka, M., Matsumoto, T., Oida, S.A. Boundary Element Method Applied to the Elastostatic Bending Problem of Beam-Stiffened Plates. Engineering Analysis with Boundary Elements. 2000. 24(10). Pp. 751–758. DOI: 10.1016/S0955-7997(00)00057-6
13. Sapountzakis, E.J., Katsikadelis, J.T. Analysis of Plates Reinforced with Beams. Computational Mechanics. 2000. 26(1). Pp. 66–74. DOI: 10.1007/s004660000156
14. Singh, D.K., Duggal S.K., Pal, P. Analysis of Stiffened Plates using FEM – A Parametric Study. International Research Journal of Engineering and Technology. 2015. 2(4). Pp. 1650–1656.
15. Troina, G.S., Cunha, M.L., Pinto, V.T., Rocha, L.A.O., Dos Santos, E.D., Fragassa, C., Isoldi, L.A. Computational Modeling and Design Constructal Theory Applied to the Geometric Optimization of Thin Steel Plates with Stiffeners Subjected to Uniform Transverse Load. Metals. 2020. 10. Pp. 1–29. DOI: 10.3390/met10020220
16. Rappaz, M., Bellet M., Deville, M. Numerical Modeling in Materials Science and Engineering. Heidelberg: Springer, 2010. DOI: 10.1007/978-3-642-11821-0
17. Steinhauser, M.O. Computational Multiscale Modeling of Fluids and Solids. Heidelberg: Springer, 2008. DOI: 10.1007/978-3-540-75117-5
18. Ansys Academic Research Mechanical, Release 19, Help System, Element Reference, ANSYS, Inc.
19. Troina, G.S., de Queiroz, J.P.T.P., Cunha, M.L., Rocha, L.A.O., dos Santos E.D., Isoldi, L.A. Verificação de modelos computacionais para placas com enrijecedores submetidas a carregamento transversal uniforme. CEREUS. 2018. 5(2). Pp. 285–298. DOI: 10.18605/2175-7275/cereus.v10n2p285-298
20. Carrijo, E.C., Paiva, J.B., Giogo, J.S. (1999). A numerical and experimental study of stiffened plates in bending. Transactions on Modelling and Simulation. 1999. 22. Pp. 12–18. DOI: 10.2495/CMEM990021

21. Bejan, A., Zane, J.P. Design in Nature: How the Constructal Law governs evolution in biology, physics, technology, and social organizations. Doubleday: New York, 2012.
22. Reis, A.H. Constructal theory: from engineering to physics, and how flow systems develop shape and structure. Applied Mechanics Reviews. 2006. 59(5). Pp. 269–281. DOI: 10.1115/1.2204075
23. Bejan, A., Lorente, S. Design with Constructal Theory, Wiley: Hoboken, 2008. DOI: 10.1002/9780470432709
24. Dos Santos, E.D., Isoldi, L.A., Gomes, M.N., Rocha, L.A.O. The Constructal Design Applied to Renewable Energy Systems. In Rincón-Mejía. E & De las Heras. A (Ed.), Sustainable Energy Technologies 1ed. Pp. 63–87. Boca Raton: CRC Press – Taylor & Francis Group, 2017. DOI: 10.1201/9781315269979
25. Lorente, S., Lee, J., Bejan, A. The "flow of stresses" concept: the analogy between mechanical strength and heat convection. International Journal of Heat and Mass Transfer. 2010. 53. Pp. 2963–2968. DOI: 10.1016/j.ijheatmasstransfer.20-10.03.038
26. Isoldi, L.A., Real, M.V., Correia, A.L.G., Vaz, J., Dos Santos, E.D., Rocha, L.A.O. Flow of Stresses: Constructal Design of Perforated Plates Subjected to Tension or Buckling. In Rocha, L.A.O., Lorente, S., Bejan, A. (Ed.), Constructal Law and the Unifying Principle of Design – Understanding Complex Systems 1ed. Pp. 195–127. New York: Springer, 2013. DOI: 10.1007/978-1-4614-5049-8_12
27. Helbig, D., Da Silva, C.C.C., Real, M.V., Dos Santos, E.D., Isoldi, L.A., Rocha, L.A.O. Study About Buckling Phenomenon in Perforated Thin Steel Plates Employing Computational Modeling and Constructal Design Method. Latin American Journal of Solids and Structures. 2016. 13. Pp. 1912–1936. DOI: 10.1590/1679-78252893
28. Da Silva, C.C.C., Helbig, D., Cunha, M.L., Dos Santos, E.D., Rocha, L.A.O., Real, M.V., Isoldi, L.A. Numerical buckling analysis of thin steel plates with centered hexagonal perforation through constructal design method. Journal of the Brazilian Society of Mechanical Sciences and Engineering. 2019. 41(8). Pp. 309–1-309–18. DOI: 10.1007/s40430-019-1815-7
29. Lima, J.P.S., Rocha, L.A.O., Dos Santos, E.D., Real, M.V., Isoldi, L.A. Constructal design and numerical modeling applied to stiffened steel plates submitted to elasto-plastic buckling. Proceedings of the Romanian Academy Series A-Mathematics Physics Technical Sciences Information Science. 2018. 19. Pp. 195–200.
30. Lima, J.P.S., Cunha, M.L., dos Santos, E.D. Rocha, L.A.O., Real, M.V., Isoldi, L.A. Constructal Design for the ultimate buckling stress improvement of stiffened plates submitted to uniaxial compressive load. Engineering Structures. 2020. 203. 109883. DOI: 10.1016/j.engstruct.2019.109883
31. De Queiroz, J., Cunha, M.L., Pavlovic, A., Rocha, L.A.O, Dos Santos, E.D., Troina, G.S., Isoldi, L.A. Geometric Evaluation of Stiffened Steel Plates Subjected to Transverse Loading for Naval and Offshore Applications. Journal of Marine Science and Engineering. 2019. 7(1). Pp. 7–18. DOI: 10.3390/jmse7010007
32. Pinto, V.T., Cunha, M.L., Troina, G.S., Martins, K.L., dos Santos, E.D., Isoldi, L.A., Rocha, L.A.O. Constructal design applied to geometrical evaluation of rectangular plates with inclined stiffeners subjected to uniform transverse load. Research on Engineering Structures and Materials. 2019. 5. Pp. 379–392. DOI: 10.17515resm2019.118ms0215
33. Mardanpour, P., Izadpanahi, E., Rastkar, S., Lorente, S., Bejan, A. Constructal design of aircraft: flow of stresses and aeroelastic stability. AIAA Journal. 2019. DOI: 10.2514/1.J057183
34. Izadpanahi, E., Moshtaghzadeh, M., Radnezhad, H.R., Mardanpour, P. Constructal approach to design of wing cross-section for better flow of stresses. AIAA Journal. 2020. DOI: 10.2514/6.2020-0275

Contacts:

Vinicius Pinto, viniciustorreseng@gmail.com
Marcelo Cunha, marcelolamcunha@hotmail.com
Kaue Martins, leaodoparque@gmail.com
Luiz Rocha, luizor@unisinos.br
Elizaldo Dos Santos, elizaldosantos@furg.br
Liercio Isoldi, liercioisoldi@gmail.com